depends on extracellular matrix components. Transplant. Proc. 37:4587–4588; 2005.
12. Ohashi, K.; Kay, M. A.; Yokoyama, T.; Kuge, H.; Kanehiro, H.; Hisanaga, M.; Ko, S.; Nagao, S.; Sho, M.; Nakajima, Y. Stability and repeat regeneration potential of the engineered liver tissues under the kidney capsule in mice. Cell Transplant. 14:621–627; 2005.
13. Ohashi, K.; Marion, P. L.; Nakai, H.; Meuse, L.; Cullen, J. M.; Bordier, B. B.; Schwall, R.; Greenberg, H. B.; Glenn, J. S.; Kay, M. A. Sustained survival of human hepatocytes in mice: A model for in vivo infection with human hepatitis B and hepatitis delta viruses. Nat. Med. 6:327–331; 2000.
14. Ohashi, K.; Park, F.; Kay, M. A. Hepatocyte transplantation: Clinical and experimental application. J. Mol. Med. 79:617–630; 2001.
15. Ohashi, K.; Tatsumi, K.; Utoh, R.; Takagi, S.; Shima, M.; Okano, T. Engineering liver tissues under the kidney capsule site provides therapeutic effects to hemophilia B mice. Cell Transplant. 19:807–813; 2010.
16. Ohashi, K.; Waugh, J. M.; Dake, M. D.; Yokoyama, T.; Kuge, H.; Nakajima, Y.; Yamanouchi, M.; Naka, H.; Yoshioka, A.; Kay, M. A. Liver tissue engineering at extrahepatic sites in mice as a potential new therapy for genetic liver diseases. Hepatology 41:132–140; 2005.
17. Ohashi, K.; Yokoyama, T.; Yamato, M.; Kuge, H.; Kanehiro, H.; Tsutsumi, M.; Amanuma, T.; Iwata, H.; Yang, J.; Okano, T.; Nakajima, Y. Engineering functional two- and three-dimensional liver systems in vivo using hepatic tissue sheets. Nat. Med. 13:880–885; 2007.
18. Pipe, S. W.; High, K. A.; Ohashi, K.; Ural, A. U.; Lillicrap, D. Progress in the molecular biology of inherited bleeding disorders. Haemophilia S3:130–137; 2008.
19. Sandgren, E. P.; Palmiter, R. D.; Heckel, J. L.; Daugherty, C. C.; Brinster, R. L.; Degan, J. L. Complete hepatic regeneration after somatic deletion of an albumin-plasminogen activator transgene. Cell 66:245–256; 1991.
20. Stephenne, X.; Najimi, M.; Sibille, C.; Nassogne, M. C.; Smets, F.; Sokal, E. M. Sustained engraftment and tissue enzyme activity after liver cell transplantation for argininosuccinate lyase deficiency. Gastroenterology 130:1317–1323; 2006.
21. Strom, S. C.; Bruzzone, P.; Cai, H.; Ellis, E.; Lehmann, T.; Mitamura, K.; Miki, T. Hepatocyte transplantation: Clinical experience and potential for future use. Cell Transplant. 15:S105–110; 2006.
22. Tateno, C.; Yoshizane, Y.; Saito, N.; Kataoka, M.; Utoh, R.; Yamasaki, C.; Tachibana, A.; Soeno, Y.; Asahina, K.; Hino, H.; Asahara, T.; Yokoi, T.; Furukawa, T.; Yoshizato, K. Near completely humanized liver in mice shows human-type metabolic responses to drugs. Am. J. Pathol. 165:901–912; 2004.
23. Tatsumi, K.; Ohashi, K.; Kataoka, M.; Tateno, C.; Shibata, M.; Naka, H.; Shima, M.; Hisanaga, M.; Kanehiro, H.; Okano, T.; Yoshizato, K.; Nakajima, Y. Successful in vivo propagation of factor IX-producing hepatocytes in mice: Potential for cell-based therapy for haemophilia B. Thromb. Haemost. 99:883–891; 2008.
24. Tatsumi, K.; Ohashi, K.; Shima, M.; Nakajima, Y.; Okano, T.; Yoshioka, A. Therapeutic effects of hepatocyte transplantation on hemophilia B. Transplantation 86:167–170; 2008.
25. Witek, R. P.; Fisher, S. H.; Pertersen, B. E. Monocrotaline, an alternative to retrorsine-based hepatocyte transplantation in rodents. Cell Transplant. 14:41–47; 2005.
26. Wu, Y. M.; Kao, C. Y.; Huang, Y. J.; Yu, I. S.; Lee, H. S.; Lai, H. S.; Lee, P. H.; Lin, C. N.; Lin, S. W. Genetic modification of donor hepatocytes improves therapeutic efficacy for hemophilia B in mice. Cell Transplant. 19: 1169–1180; 2010.
27. Yamada, N.; Okano, T.; Sakai, H.; Karikusa, F.; Sawasaki, Y.; Sakurai, Y. Thermo-responsive polymeric surfaces; control of attachment and detachment of cultured cells. Makromol. Chem. Rapid Commun. 11:571–576; 1990.
28. Yang, J.; Yamato, M.; Sekine, H.; Sekiya, S.; Tsuda, Y.; Ohashi, K.; Shimizu, T.; Okano, T. Tissue engineering using laminar cellular assemblies. Adv. Mater. 21:1–6; 2009.
29. Yang, J.; Yamato, M.; Shimizu, T.; Sekine, H.; Ohashi, K.; Kanzaki, M.; Ohki, T.; Nishida, K.; Okano, T. Reconstruction of functional tissues with cell sheet engineering. Biomaterials 28:5033–5043; 2007.
30. Yokoyama, T.; Ohashi, K.; Kuge, H.; Kanehiro, H.; Iwata, H.; Yamato, M.; Nakajima, Y. In vivo engineering of metabolically active hepatic tissues in a neovascularized subcutaneous cavity. Am. J. Transplant. 6:50–59; 2006.
31. Yoshitsugu, H.; Nishimura, M.; Tateno, C.; Kataoka, M.; Takahashi, E.; Soeno, Y.; Yoshizato, K.; Yakoi, T.; Naito, S. Evaluation of human CYP1A2 and CYP3A4 mRNA expression in hepatocytes from chimeric mice with humanized liver. Drug Metab. Pharmacokinet. 21:465–474; 2006.

HEPATOLOGY
Official Journal of the American Association for the Study of Liver Diseases

Severe Necroinflammatory Reaction Caused by Natural Killer Cell-Mediated Fas/Fas Ligand Interaction and Dendritic Cells in Human Hepatocyte Chimeric Mouse

Akihito Okazaki,[1,2] Nobuhiko Hiraga,[1,2] Michio Imamura,[1,2] C. Nelson Hayes,[1,2,3] Masataka Tsuge,[1,2] Shoichi Takahashi,[1,2] Hiroshi Aikata,[1,2] Hiromi Abe,[1,2,3] Daiki Miki,[1,2,3] Hidenori Ochi,[1,2,3] Chise Tateno,[2,4] Katsutoshi Yoshizato,[2,4] Hideki Ohdan,[2,5] and Kazuaki Chayama[1,2,3]

The necroinflammatory reaction plays a central role in hepatitis B virus (HBV) elimination. Cluster of differentiation (CD)8-positive cytotoxic T lymphocytes (CTLs) are thought to be a main player in the elimination of infected cells, and a recent report suggests that natural killer (NK) cells also play an important role. Here, we demonstrate the elimination of HBV-infected hepatocytes by NK cells and dendritic cells (DCs) using urokinase-type plasminogen activator/severe combined immunodeficiency mice, in which the livers were highly repopulated with human hepatocytes. After establishing HBV infection, we injected human peripheral blood mononuclear cells (PBMCs) into the mice and analyzed liver pathology and infiltrating human immune cells with flow cytometry. Severe hepatocyte degeneration was observed only in HBV-infected mice transplanted with human PBMCs. We provide the first direct evidence that massive liver cell death can be caused by Fas/Fas ligand (FasL) interaction provided by NK cells activated by DCs. Treatment of mice with anti-Fas antibody completely prevented severe hepatocyte degeneration. Furthermore, severe hepatocyte death can be prevented by depletion of DCs, whereas depletion of CD8-positive CTLs did not disturb the development of massive liver cell apoptosis. ***Conclusion:*** **Our findings provide the first direct evidence that DC-activated NK cells induce massive HBV-infected hepatocyte degeneration through the Fas/FasL system and may indicate new therapeutic implications for acute severe/fulminant hepatitis B.** (HEPATOLOGY 2012;56:555-566)

Between 4% and 32% of fulminant hepatitis cases, characterized by acute massive hepatocyte degeneration and subsequent development of hepatic encephalopathy and liver failure, are caused by acute hepatitis B virus (HBV) infection.[1] Host[2] and viral factors[3] may influence the development of fulminant hepatitis, but these factors have not been fully elucidated.

Innate and adaptive immunity both play a role in the elimination of viral infections. In the innate immune response, cytoplasmic and membrane-bound receptors recognize viruses and induce interferon (IFN)-β production, which, in turn, up-regulates IFN-α and induces an antiviral state in surrounding cells.[4] In the adaptive immune response, viruses are recognized by dendritic cells (DCs), which activate cluster of differentiation (CD)8-positive T cells to reduce viral replication through cytolytic[5] and noncytolytic mechanisms.[6] The role of immune cells, especially HBV-specific cytotoxic T lymphocytes (CTLs), is crucial in the

Abbreviations: APC, allophycocyanin; asialo GM1, ganglio-N-tetraosylceramide; CD, cluster of differentiation; CHB, chronic hepatitis B; CTLs, cytotoxic T lymphocytes; DC, dendritic cell; FasL, Fas ligand; FHB, fulminant hepatitis B; HBcAg, hepatitis B core antigen; HBsAg, hepatitis B surface antigen; HBV, hepatitis B virus; HLA, human leukocyte antigen; HSA, human serum albumin; IFN, interferon; IP, intraperitoneally; ISG, interferon-stimulated gene; mAb, monoclonal antibody; mDC, myeloid DC; mRNA, messenger RNA; NK, natural killer; PBMCs, peripheral blood mononuclear cells; PCR, polymerase chain reaction; pDC, plasmacytoid DC; SCID, severe combined immunodeficiency; TUNEL, terminal deoxynucleotidyl transferase dUTP nick end labeling; uPA, urokinase-type plasminogen activator.

From the [1]Department of Medicine and Molecular Science, Division of Frontier Medical Science, Programs for Biomedical Research, Graduate School of Biomedical Sciences, Hiroshima University, Hiroshima, Japan; [2]Liver Research Project Center, Hiroshima University, Hiroshima, Japan; [3]Laboratory for Digestive Diseases, Center for Genomic Medicine, RIKEN, Hiroshima, Japan; [4]PhoenixBio Co., Ltd., Higashi-Hiroshima, Japan; and [5]Department of Surgery, Division of Frontier Medical Science, Programs for Biomedical Research, Graduate School of Biomedical Science, Hiroshima University, Hiroshima, Japan.

Received August 16, 2011; accepted February 4, 2012.

This study was supported, in part, by a Grant-in-Aid for Scientific Research from the Japanese Ministry of Labor, Health, and Welfare.

development of fulminant hepatitis.[7,8] CTLs can kill target cells using two distinct lytic pathways: the degranulation pathway, in which perforin is used to puncture the membranes of infected cells, and the Fas-based pathway, in which the interaction between Fas ligand (FasL) expressed on cytolytic lymphocytes and Fas on target cells triggers apoptosis and target cell death.[9] However, the role of innate immune cells, especially natural killer (NK) cells, in fulminant hepatitis remains obscure. NK cells have recently been reported to contribute to the pathogenesis of human hepatitis and animal models of liver injury.[10,11] Replication of HBV is host cell dependent, and the study of cellular immune response in hepatitis B has long been hampered by the lack of a small animal model that supports the replication of HBV and elimination of infected cells by immune response. Before the advent of human hepatocyte chimeric mice,[12,13] only chimpanzees had been used as a model for HBV infection and inflammation, although fulminant hepatitis B (FHB) had never been reported, and severe liver inflammation is rare in chimpanzees.[14] We previously established an HBV-infection animal model using chimeric mice, in which the livers were extensively repopulated with human hepatocytes.[15-17] In this study, we attempted to establish an animal model of HBV-infected human hepatocytes with human immunity by transplanting human peripheral mononuclear cells (PBMCs) to HBV-infected human hepatocyte chimeric mice.

Materials and Methods

Generation of Human Hepatocyte Chimeric Mice. Generation of the urokinase-type plasminogen activator (uPA)$^{+/+}$/severe combined immunodeficiency (SCID)$^{+/+}$ mice and transplantation of human hepatocytes with human leukocyte antigen (HLA)-A0201 were performed as described previously.[15,16] All mice were transplanted with frozen human hepatocytes obtained from the same donor. Infection, extraction of serum samples, and euthanasia were performed under ether anesthesia. Concentration of human albumin, which is correlated with the repopulation index,[15] was measured in mice as described previously.[16] All animal protocols described in this study were performed in accord with the *Guide for the Care and Use of Laboratory Animals* and the local committee for animal experiments, and the experimental protocol was approved by the Ethics Review Committee for Animal Experimentation of the Graduate School of Biomedical Sciences at Hiroshima University (Hiroshima, Japan).

Human Serum Samples. Human serum samples, containing high titers of genotype C HBV DNA (5.3×10^6 copies/mL), were obtained from patients with chronic hepatitis who provided written informed consent. Individual serum samples were divided into aliquots and stored in liquid nitrogen. Six weeks after hepatocyte transplantation, chimeric mice were injected intravenously with 50 μL of HBV-positive human serum.

Analysis of HBV. DNA was extracted using SMITEST (Genome Science Laboratories, Tokyo, Japan) and dissolved in 20 μL of H_2O. HBV DNA was measured by real-time polymerase chain reaction (PCR) using a light cycler (Roche, Mannheim, Germany). Primers used for amplification were 5′-TTTGGGCATGGACATTGAC-3′ and 5′-GGTGA ACAATGTTCCGGAGAC-3′. Amplification conditions included initial denaturation at 95°C for 10 minutes, followed by 45 cycles of denaturation at 95°C for 15 seconds, annealing at 58°C for 5 seconds, and extension at 72°C for 6 seconds. The lower detection limit of this assay was 300 copies.

Preparation of Human Blood Mononuclear Cells and Transplantation of Human PBMCs Into Human Hepatocyte Chimeric Mice. PBMCs were isolated from healthy blood donors with HLA-A0201 and successfully vaccinated with recombinant yeast-derived hepatitis B surface antigen (HBsAg) vaccine (Bimmugen; Chemo-Sero Therapeutic Institute, Kumamoto, Japan) using Ficoll-Hypaque density gradient centrifugation. Neither monocytes nor macrophages were observed in the isolated PBMCs (Supporting Fig. 1). PBMCs isolated from 3 healthy, unvaccinated blood donors were also transplanted. Eight weeks after HBV inoculation, human PBMCs were transplanted into human hepatocyte chimeric mice. To deplete mouse NK cells and prevent the elimination of human PBMCs from human hepatocyte

Address reprint requests to: Kazuaki Chayama, M.D., Ph.D., Department of Medical and Molecular Science, Division of Frontier Medical Science, Programs for Biomedical Research, Graduate School of Biomedical Science, Hiroshima University, 1-2-3 Kasumi, Minami-ku, Hiroshima 734-8551, Japan. E-mail: chayama@hiroshima-u.ac.jp; fax: +81-82-255-6220.

View this article online at wileyonlinelibrary.com.
DOI 10.1002/hep.25651
Potential conflict of interest: The authors have no conflicts to disclose.
Additional Supporting Information may be found in the online version of this article.

chimeric mice, 200 μL of phosphate-buffered saline, containing 120 μL of anti–ganglio-N-tetraosylceramide (asialo GM1) antibody (Wako, Osaka, Japan), were administered intraperitoneally (IP) 1 day before (day 0; Fig. 1) the initial IP transplantation (day 1) of human PBMC. Then, 10 μL/g of liposome-encapsulated clodronate (Sigma-Aldrich, St. Louis, MO) were also administered 4 days before PBMC transplantation (day −2) to deplete mouse macrophages and DC cells. The second PBMC administration (4×10^7 cells/mouse) was performed 2 days after the initial administration (day 3).

To assess the effect of the depletion of human DC, NK, or CD8-positive CTL cells from administered PBMCs on hepatitis formation, the BD IMag separation system (BD Biosciences, Franklin Lakes, NJ) was used. Alternatively, mice were treated with an IP administration of clodronate, as described above, 1 day before PBMC transplantation.

To analyze the effect of inhibition of the Fas/FasL system, IFN-γ, IFN-α, antihuman FasL monoclonal antibody (mAb) (1.5 mg/mouse; R&D Systems, Minneapolis, MN), antihuman IFN-γ mAb (1.5 mg/mouse; R&D Systems), and antihuman IFN-α mAb (1.5 mg/mouse; PBL Biomedical Laboratories, Piscataway, NJ) were injected 1 day before transplantation of human PBMCs.

Flow Cytometry. Reconstructed human PBMC proliferation in mice was determined by flow cytometry with the following mAbs used for PBMC surface staining: allophycocyanin (APC)-H7 antihuman CD3 (clone SK7); APC-conjugated anti-CD4 (clone SK); BD Horizon V450 antihuman CD8 (clone RPA-T8); APC-conjugated antihuman CD11c (clone B-ly6); HU HRZN V500 MAB-conjugated antihuman CD45 (clone H130); Alexa Fluor 488–conjugated antihuman CD56 (clone B159); PerCP-Cy5.5 antihuman CD123 (clone 7G3); fluorescein isothiocyanate–conjugated Lineage cocktail 1 (Lin-1) (anti-CD3, CD14, CD16, CD19, CD20, and CD56); APC-H7 antihuman HLA-DR (clone L243); phycoerythrin (PE)-conjugated antihuman FasL (clone NOK-1); and biotin-conjugated antimouse H-2D^b (clone KH95). The biotinylated mAbs were visualized using PE-Cy7-streptavidin. Each of the above mAbs were purchased from BD Biosciences. PE-conjugated HBV core-derived immunodominant CTL epitope (HBcAg93)[18] (Medical & Biological Laboratories Co., Ltd., Nagoya, Japan). Dead cells identified by light scatter and propidium iodide staining were excluded from the analysis. Flow cytometry was performed using a FACSAria II flow cytometer (BD Biosciences), and results were analyzed with FlowJo software (Tree Star, Inc., Ashland, OR).

DCs can be classified into two main subsets: plasmacytoid DCs (pDCs) and myeloid DCs (mDCs).[19,20] pDCs were defined as CD45$^+$Lin-1$^-$HLA-DR$^+$CD123$^+$ cells, whereas mDCs were defined as CD45$^+$ Lin-1$^-$HLA-DR$^+$CD11c$^+$ cells.

Histochemical Analysis of Mouse Liver and Terminal Deoxynucleotidyl Transferase dUTP Nick End Labeling Assay. Histochemical analysis and immunohistochemical staining using an antibody against human serum albumin (HSA; Bethyl Laboratories, Inc., Montgomery, TX), an antibody against hepatitis B core antigen (HBcAg) (Dako Diagnostika, Hamburg, Germany) and antibody against Fas (BD Biosciences, Tokyo, Japan) were performed as described previously.[16] Immunoreactive materials were visualized using a streptavidin-biotin staining kit (Histofine SAB-PO kit; Nichirei, Tokyo, Japan) and diainobenzidine. For the terminal deoxynucleotidyl transferase dUTP nick end labeling (TUNEL) assay in sliced tissues, we used an *in situ* cell death detection kit (POD; Roche Diagnostics Japan, Tokyo, Japan).

Dissection of Mouse Livers and Isolation of RNA and Measurement of Messenger RNAs of Fas by Reverse-Transcription PCR. Mice were sacrificed by anesthesia with diethyl ether, and livers were excised, dissected into small sections, and then snap-frozen in liquid nitrogen. Total RNA was extracted from cell lines using the RNeasy Mini Kit (Qiagen, Valencia, CA). One microgram of each RNA sample was reverse transcribed with ReverseTra Ace (Toyobo Co., Tokyo, Japan) and Random Primer (Takara Bio Inc., Kyoto, Japan). We analyzed the messenger RNA (mRNA) levels of Fas by reverse-transcription PCR, as previously reported, using Fas forward primer 5′-GGGCATCTGGACCCTCCTA-3′ and Fas reverse primer 5′- GGCATTAACACTTTTGGACGATAA-3′.

Statistical Analysis. mRNA expression levels of Fas and interferon-stimulated genes (ISGs) were compared using Mann-Whitney's U test and unpaired *t* tests. A *P* value less than 0.05 was considered statistically significant.

Results

Establishment of an Animal Model of Fulminant Hepatitis Using HBV-Infected Human Hepatocyte Chimeric Mice and Human PBMC Transplantation. Administration of 2×10^7 PBMCs twice after suppression of mice NK cells by anti–asialo GM1 antibody[21] and macrophages and DCs by liposome-encapsulated clodronate[22] before transplantation

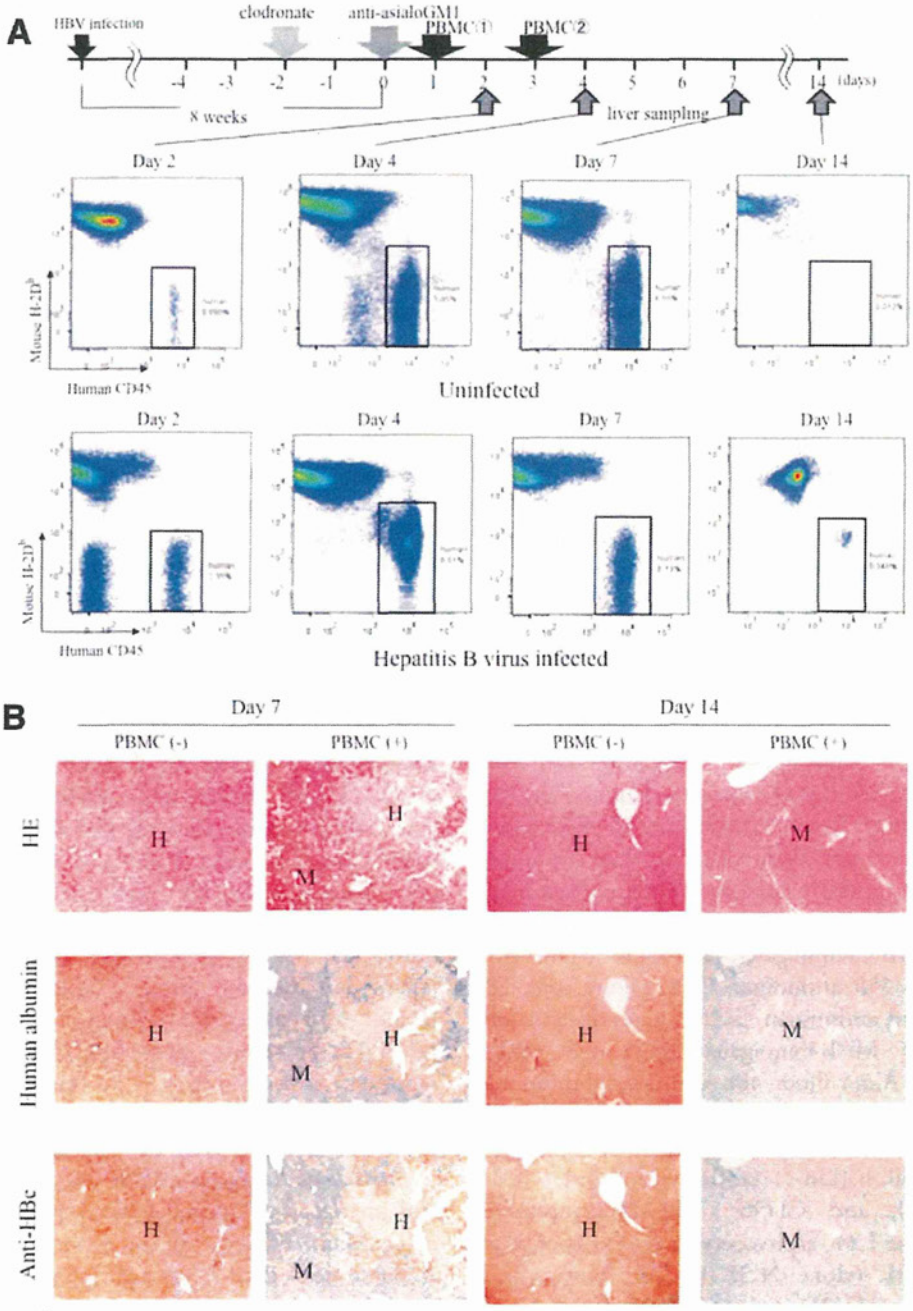

Fig. 1. Establishment of human PBMC chimerism in human hepatocyte chimeric mice. (A) Experimental protocol to establish chimerism and liver sampling is shown at the top of the figure (see Materials and Methods). Scheduling of administration of HBV-positive serum, clodronate, and anti-asialo GM1 antibody and liver sampling by scarification are shown by arrows. Liver mononuclear cells isolated from uninfected (upper panel) and HBV-infected (lower panel) human hepatocyte chimeric mice transplanted with human PBMCs were separated with antibodies for human CD45 and mouse H-2D^b and were analyzed by flow cytometry. Percentage of human mononuclear cells is shown in each panel. Representative figures of two experiments with similar results are shown. (B) Histological analysis of livers of HBV-infected mice. Liver samples obtained from mice with or without human PBMCs at weeks 9 (day 7) and 10 (day 14) were stained with hematoxylin and eosin staining (HE), anti-human albumin antibody, or anti-hepatitis B core antibody. Regions are shown as human (H) and mouse (M) hepatocytes, respectively (original magnification, 40×). (C) Time course of human albumin concentration (upper panel) and HBV DNA titer (lower panel) in mouse serum. Time course of 4 HBV-infected mice transplanted with human PBMCs, 3 HBV-infected mice without human PBMC transplantation, and 4 uninfected mice transplanted with human PBMC are shown. (D) Time course of human albumin concentration (upper panel) and HBV DNA titer (lower panel) in mice. Mice with or without HBV-infection were transplanted with PBMCs obtained from 3 healthy donors who were not vaccinated against hepatitis B.

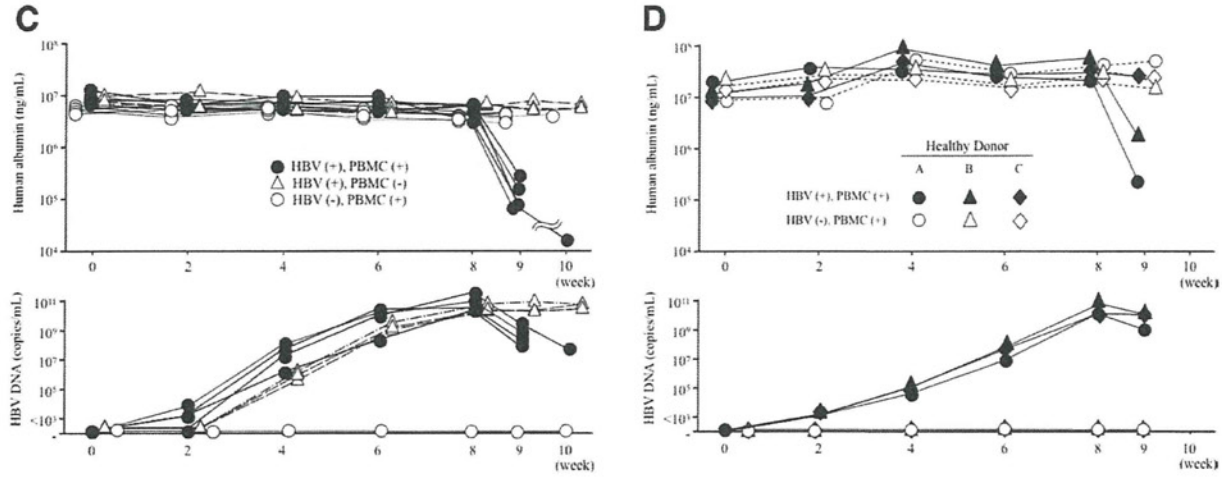

Fig. 1.

enabled us to establish a human PBMC chimerism in uPA-SCID mice. We observed an up to 7% human mononuclear cell chimerism among the liver-resident mononuclear cells of uninfected and HBV-infected mice 2-14 days after the initial injection of PBMC (Fig. 1A; Table 1). Chimerism was most prominent 4 days after initial PBMC administration and almost undetectable by day 14 (Fig. 1A). Histological examination of chimeric mice livers showed extensive human liver cell death, comparable to the massive liver cell death observed in fulminant hepatitis, only in HBV-infected and PBMC-treated mice liver (Fig. 1B). Human hepatocytes were almost completely eliminated and replaced by human albumin-negative mouse hepatocytes at days 7 and 14. Consistent with these histological changes, we observed a rapid decline of HSA levels and HBV DNA only in HBV-infected and PBMC-treated mice (Fig. 1C). The decline of mice HSA levels and HBV DNA was also observed in 2 of 3 HBV-infected mice transplanted with PBMCs isolated from healthy blood donors without HBsAg vaccination (Fig. 1D and Supporting Fig. 2).

Analysis of Liver-Infiltrating Human Lymphocytes Necessary to Establish Massive Hepatocyte Degeneration. We then analyzed liver-infiltrating cells with flow cytometry. Unexpectedly, we did not detect CD8-positive and tetramer-positive CTLs, as reported previously (Fig. 2A). Instead, we observed substantial numbers of CD3-negative and CD56-positive NK cells (Fig. 2B) and small numbers of pDCs and mDCs (Fig. 2C). The majority of NK cells of HBV-infected mice were FasL positive (Fig. 2D). In contrast, such FasL-positive NK cells were not detected in uninfected

Table 1. Analysis of Liver-Infiltrating Cells by Flow Cytometry

	HBV Infected				Uninfected			
Day	No.	Chimerism (%)	Human NK (%)	Fas (+) NK (%)	No.	Chimerism (%)	Human NK (%)	FasL (+) NK (%)
2	1	1.77	2.51	0	1	0.59	12.8	0
	2	2.35	3.02	0.143	2	0.774	58.8	1.1
4	3	6.81	30.7	80.1	3	5.95	42.7	0.678
	4	1.08	68.7	94.7	4	7.11	4.98	0.027
	5	6.60	23.2	58.7	5	5.02	23.1	0.314
7	6	6.73	13.2	0.383	6	6.55	42.1	0.103
	7	5.70	12.5	2.01	7	1.24	13.6	0.025
	8	1.46	3.83	0	8	2.04	1.49	4.03
14	9	0.34	ND	ND	9	0.012	ND	ND
	10	NA*	NA	NA	10	0.013	ND	ND
DCs depleted day 4	11	4.77	5	2.14	11	3.32	4.21	0.465
(by clodronate)	12	1.27	39.5	2.3	12	12.9	9.06	0
DCs depleted day 7	13	2.42	24.8	2.19	13	6.31	54.1	0.131
(by clodronate)	14	1.41	10.6	0.103	14	4.69	1.68	0.12

Abbreviations: NA, not analyzed; ND, not detectable.
*Mouse died just before liver analysis.

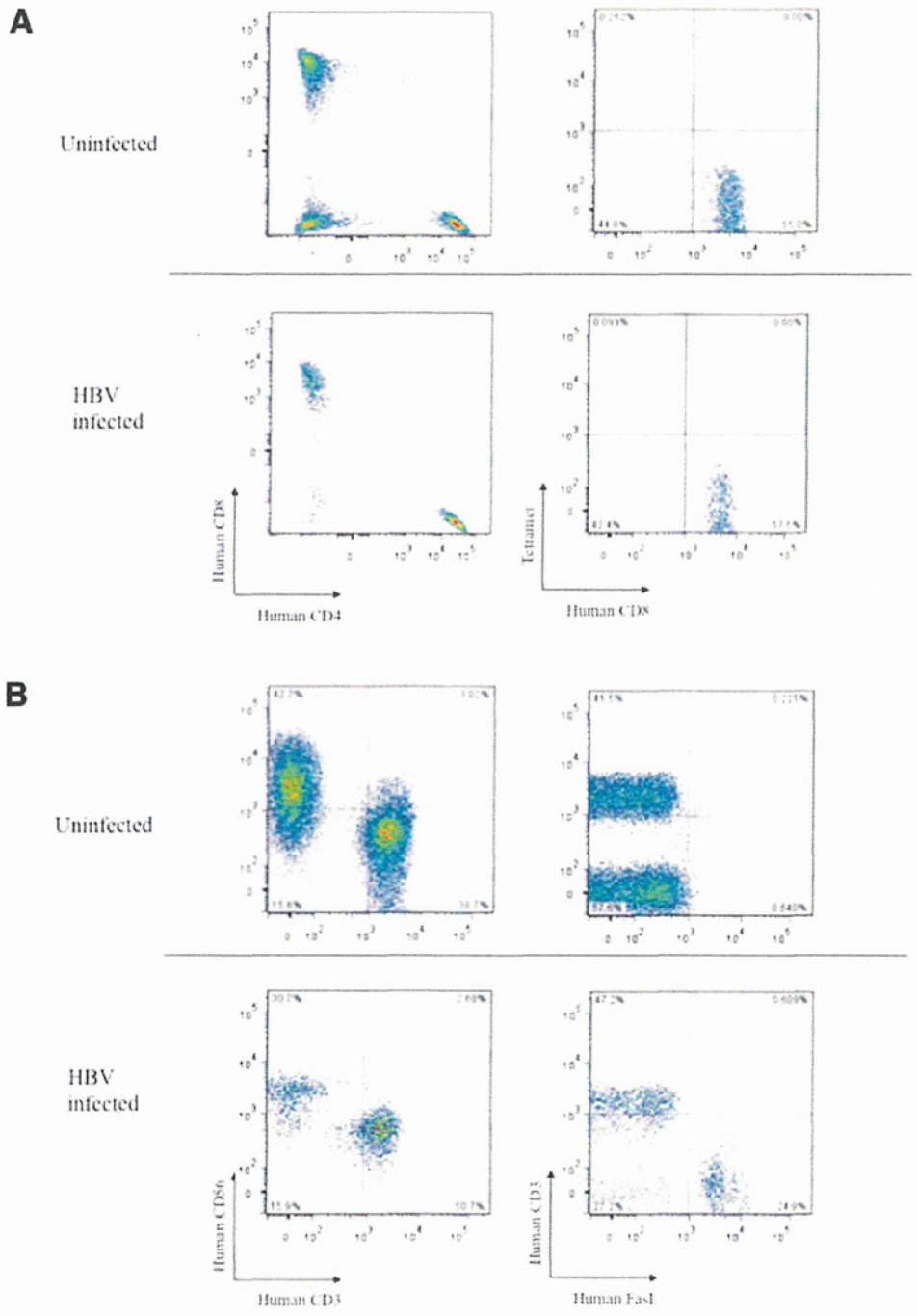

Fig. 2. Analysis of mononuclear cells isolated from day 4 chimeric mouse livers. After defining human PBMCs as mouse H-2Db-human CD45^{+} cells, we further analyzed the phenotypes of these cells. (A-C) Liver mononuclear cells of uninfected (upper panel) and HBV-infected (lower panel) mice transplanted with human PBMCs were separated with anti-human CD4 and CD8 antibody or anti-human CD8 and HLA-A2 HBcAg tetramer (A), anti-human CD3and CD56 or human CD3 and FasL (B), and anti-human HLA-DR and CD123 and HLA-DR and CD11c (C). (D) Frequency of FasL-positive cells in NK cells were analyzed in uninfected and HBV-infected mice. All figures are representative of two experiments with similar results.

mice livers (Table 1; Fig. 2D), suggesting that these NK cells were activated in HBV-infected mice. These activated NK cells and DCs were detectable in mice livers only 4 days after the initial PBMC injection, but were undetectable after 2 and 7 days (Supporting Figs. 3 and 4, respectively).

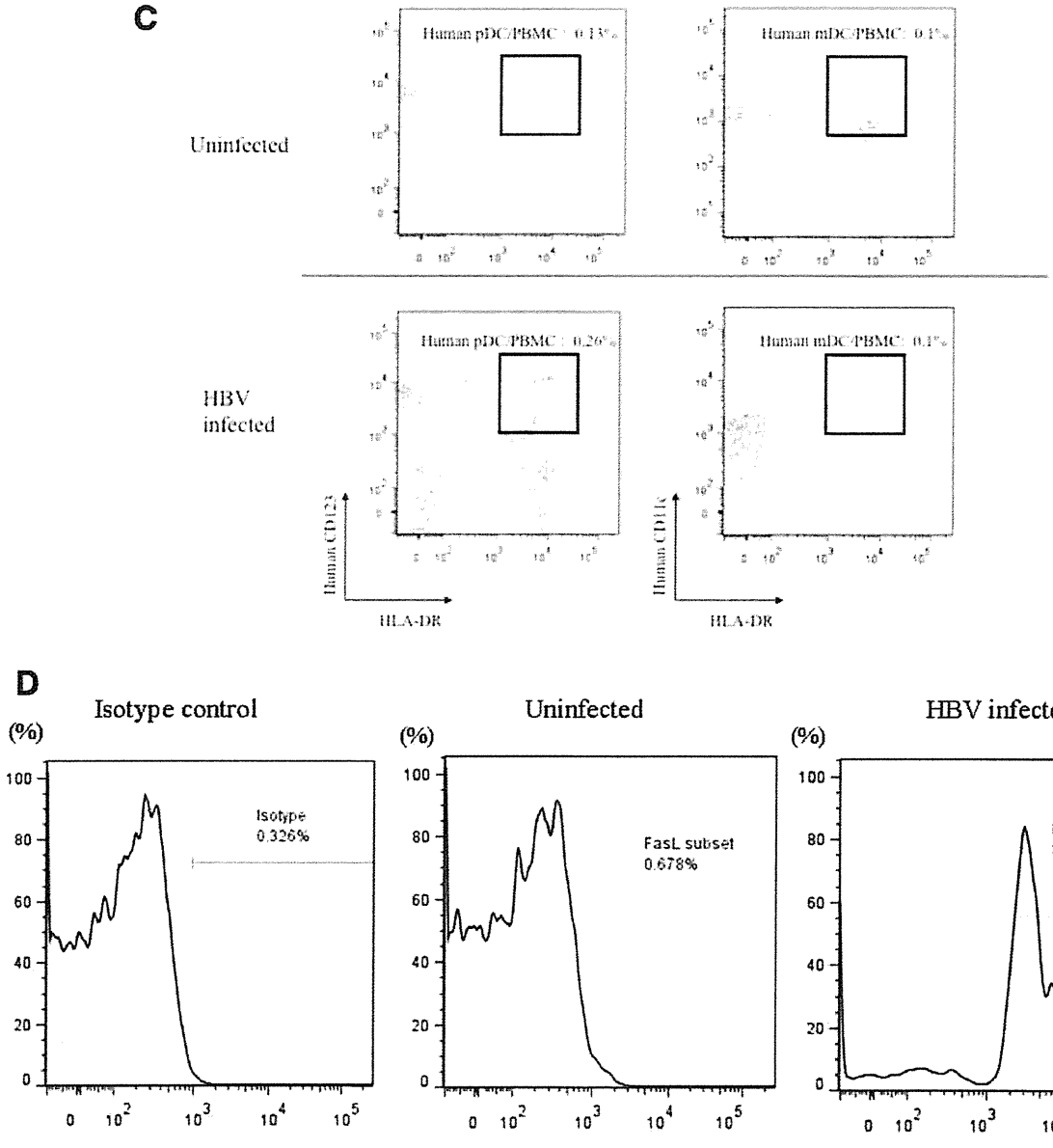

Fig. 2.

Effect of DC Depletion on Establishment of Massive Hepatocyte Degeneration. To confirm the necessity of both DCs and NK cells to complete hepatocyte destruction, we depleted DCs or NK cells with negative selection using antibody-coated magnetic beads before the administration of PBMC. Depletion of either DCs or NK cells completely abolished the decline of human albumin as well as HBV DNA (Supporting Fig. 5A). However, analysis of liver-infiltrating cells revealed that chimerism with human PBMC was poorly established in these animals, probably the result of the loss or damage of human cells by bound antibodies during separation and/or subsequent incubation in mice (Supporting Fig. 5B; Supporting Table 1).

To overcome possible confounding resulting from poor chimerism resulting in poor human hepatocyte degeneration in mice, we attempted to remove DCs from transplanted human PBMCs by alternate means. We attempted to deplete human DCs by administering clodronate 1 day before PBMC transplantation, because we thought that clodronate remaining in the mouse body would impair transplanted human DCs. As expected, we observed an almost complete elimination of DCs by this procedure without impairing

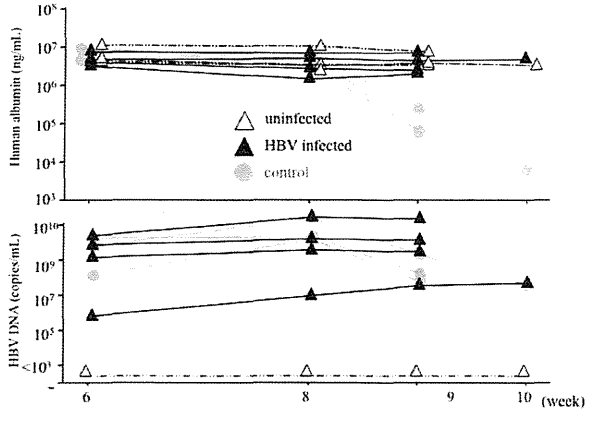

Fig. 3. Time course of mice transplanted with human PBMCs with DC depletion by clodronate 1 day before transplantation. Mice were treated with IP administration of clodronate 1 day before human PBMC transplantation. Time courses of human albumin concentration (upper panel) and HBV DNA titer (lower panel) in mouse serum are shown. Open and closed triangles correspond to 3 uninfected and 4 HBV-infected mice, respectively. Time courses of 3 mice infected with HBV and transplanted with human PBMC 3 days before transplantation (see Fig. 1C) are shown for comparison (shaded closed circle).

PBMC chimerism (Supporting Figs. 6A and 7A; Supporting Table 1). Activation of NK cells was not observed in this setting (Supporting Figs. 6B and 7B; Supporting Table 1). Depletion of DCs completely abolished the decline of both human albumin and HBV DNA (Fig. 3). Histological examination showed that hepatocyte degeneration was absent, and that there were no TUNEL-staining–positive cells (data not shown). Clodronate lyposomes may also nonspecifically deplete macrophages and monocytes in addition to DCs, but no monocytes or macrophages were observed when transplanted PBMCs were analyzed using Ficoll-Hypaque density gradient centrifugation, indicating that the clodronate administration was specifically associated with DC depletion in this study.

Analysis of Fas/FasL System in Massive HBV-Infected Hepatocyte Degeneration Model. We then assessed the importance of the Fas/FasL system and the occurrence of apoptosis in NK-cell–mediated human hepatocyte degeneration. Only HBV-infected human hepatocytes positive for HSA were positive for Fas antibody staining (Fig. 4A). TUNEL staining was also positive only in mice infected with HBV and inoculated with PBMCs (days 4 and 7). Measurement of mRNA levels in infected and uninfected livers showed that expression levels of Fas mRNA increased significantly upon HBV infection (Fig. 4B). To confirm that apoptosis of human hepatocytes was mediated by the Fas/FasL pathway and to determine whether IFN-α or IFN-γ played a role in the establishment of liver cell degeneration, we administered a blocking mAb against FasL, IFN-α, and IFN-γ 1 day before PBMC transplantation. Treatment of mice with antibody against FasL before PBMC completely abolished the decline of human albumin and HBV DNA (Fig. 5A). This abolishment of human albumin decline in mouse serum suggests that the Fas/FasL pathway almost exclusively eliminated infected hepatocytes in this model, which also suggests that Fas-mediated apoptosis could play an important role in FHB. Antibodies against IFN-α and IFN-γ inhibited IFN-induced ISG expression in mice livers (Supporting Fig. 8); however, these antibodies did not disturb the decline of HSA levels (Fig. 5A) and histological inflammation (Fig. 5B). Contact-dependent and -independent activation of NK cells by DCs has been reported previously.[23-25] Although IFN-α and IFN-γ play a role in their activation,[23,25,26] our results indicate that the effects of IFN-α are almost negligible in our experiments (Fig. 5A), suggesting that direct contact among these cells, or cytokines other than IFN-α and IFN-γ, are necessary to activate NK cells in this setting. NK cells have also been reported to exert antiviral effects by secreting IFN-γ. However, our results suggest that this mechanism does not work well in our model (Fig. 5A).

Discussion

In this study, we established a small animal model in which massive hepatocyte degeneration similar to FHB in humans is observed. Our initial attempts to detect human PBMCs in blood or any organ in transplanted mice failed even after injecting 2×10^7 cells, which is sufficient to establish human PBMC chimerism in SCID mice.[27] We assumed that failure to develop chimerism was the result of the activity of NK cells and macrophages because the activity of these cells in uPA-SCID mice is higher than in SCID mice.[28,29] Therefore, we attempted to eliminate these effects by administering clodronate and anti–asialo GM1 antibody, which are known to effectively eliminate these cells.[30,31] This assumption appears to be valid, because we were able to establish human PBMC chimerism and massive hepatocyte degeneration by suppressing these cells (Fig. 1).

HBV-specific CTLs have been reported to play an important role in eliminating the virus.[32-34] Accordingly, we attempted to detect HBV-specific CTLs in mice with massive hepatocyte degeneration. Unexpectedly, we failed to detect HBV-specific CTLs (Fig. 2A and Supporting Fig. 9) and instead found that infiltrating cells in the liver were CD3-negative NK cells

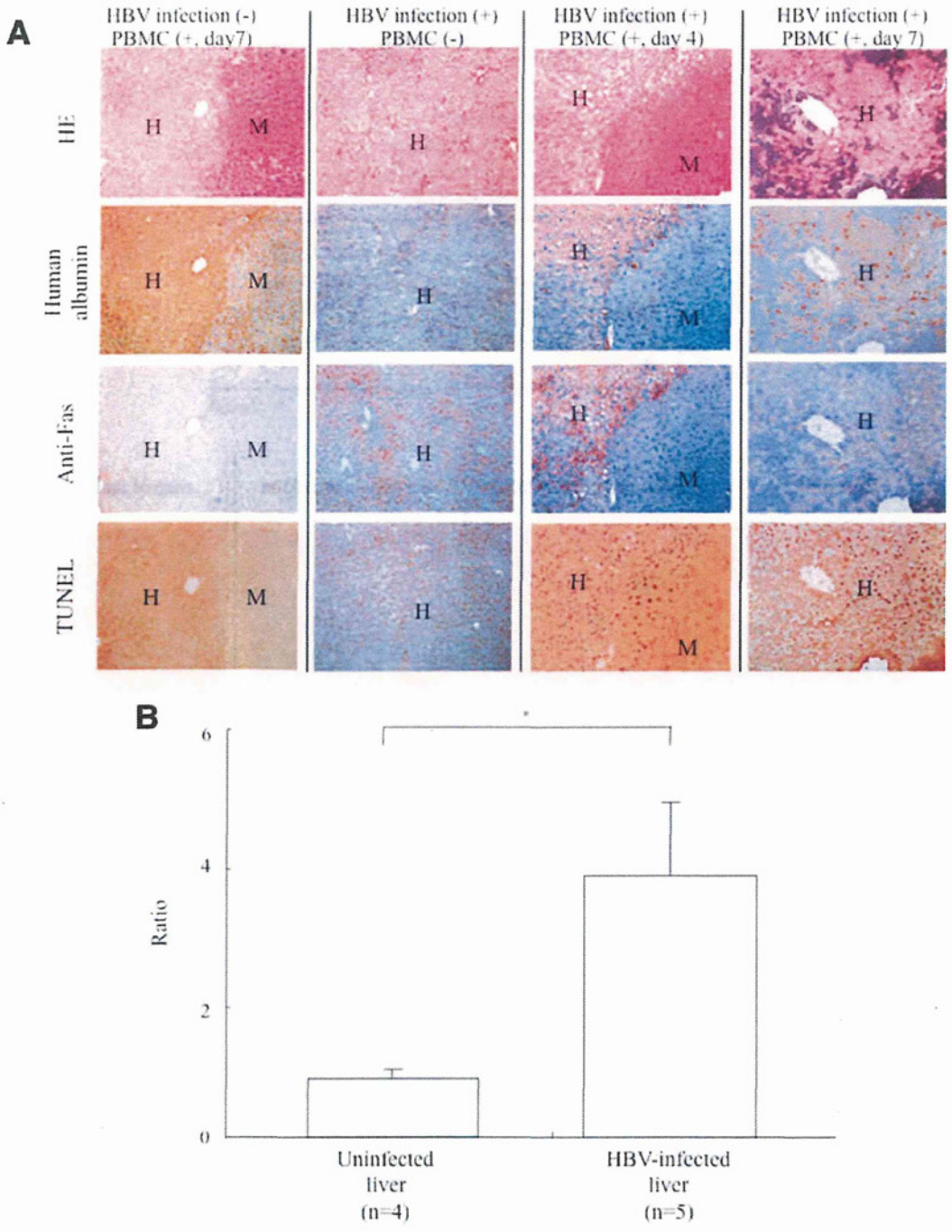

Fig. 4. Assessment of Fas expression in the liver in human hepatocyte chimeric mice. (A) Histological analysis of chimeric mice livers transplanted with human PBMCs but without HBV infection (day 7), with HBV infection but without PBMC transplantation, and with HBV infection and PBMC transplantation at days 4 and 7. Liver samples were stained with hematoxylin and eosin staining (HE), anti-human albumin antibody, anti-human Fas antibody, and TUNEL staining. Regions are shown as human (H) and mouse (M) hepatocytes, respectively (original magnification, 100×). Note that Fas antigen was expressed only in HBV-infected human hepatocytes, and TUNEL staining is only positive for HBV-infected and human PBMC-transplanted mice livers. Mouse hepatocytes were negative for all three stains. (B) Expression of Fas mRNA levels in uninfected and HBV-infected human hepatocytes. Data are represented as mean ± standard deviation. *$P < 0.001$.

(Fig. 2B,D and Supporting Fig. 10). The reason for the absence of CTLs in our experiment is unknown, but this suggests that massive hepatocyte degeneration resembling fulminant hepatitis can be caused by NK cells as a main player, and recent reports demonstrating that NK cells contribute to severe acute and

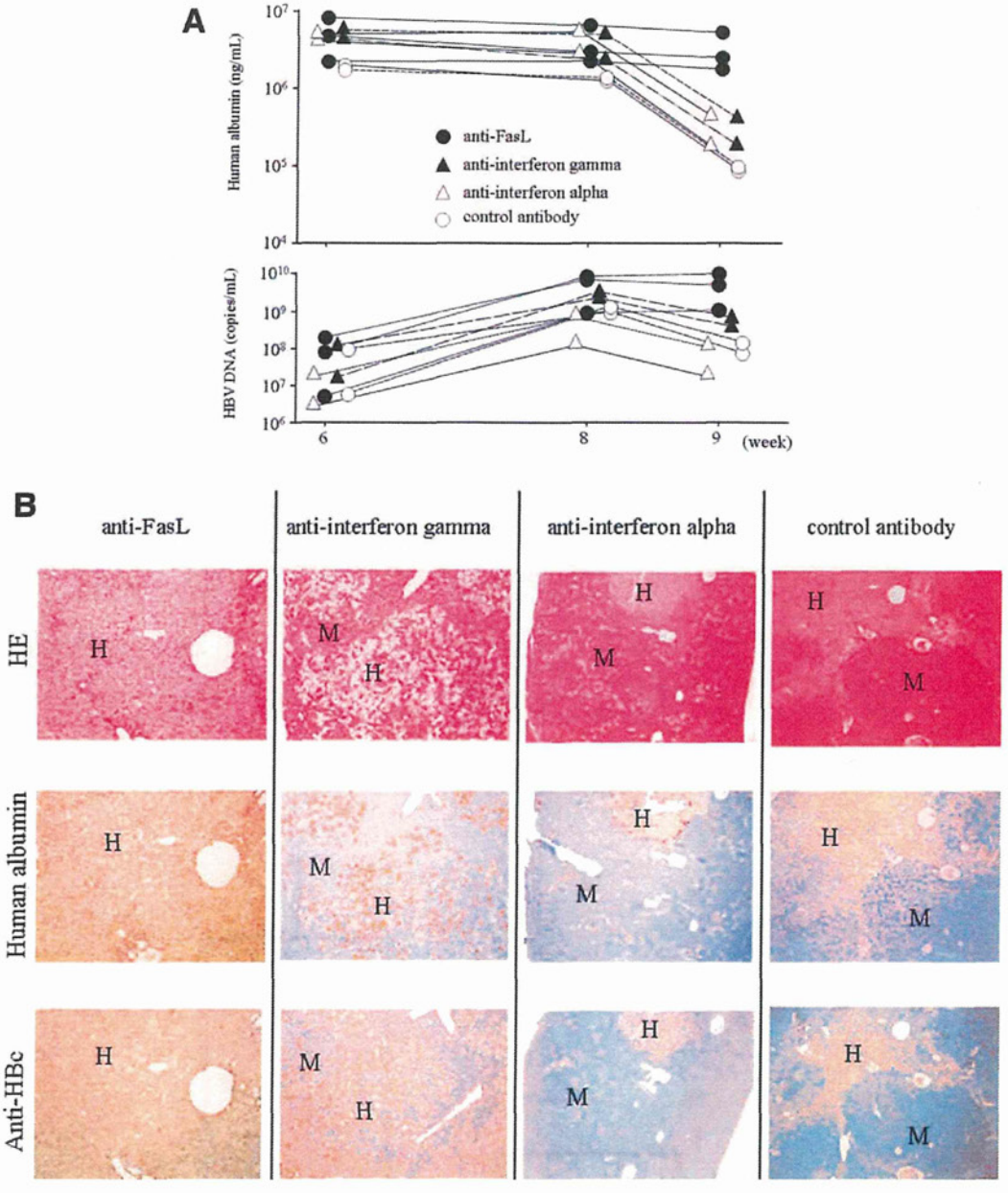

Fig. 5. Effect of anti-FasL, anti-IFN-γ and anti-IFN-α antibody administration on HSA and HBV DNA. (A) Time courses of HSA (upper panel) and HBV DNA (lower panel) before and 1 week after human PBMC transplantation are shown. Mice were pretreated with antibodies against human Fas-L, IFN-γ, and IFN-α before PBMC transplantation, as described in Materials and Methods. Isotype antibody was used as a control. (B) Histological analysis of livers of HBV-infected mice injected with anti-human FasL mAb, IFN-γ, IFN-α, and control antibody. Liver samples obtained from mice with human PBMCs at weeks 9 (day 7) were stained with hematoxylin and eosin staining (HE), antihuman albumin antibody, or antihepatitis B core antibody. Regions are shown as human (H) and mouse (M) hepatocytes, respectively (original magnification, 40×).

chronic hepatitis B (CHB) support this assertion.[11,35] We attempted to collect CTLs from HBV-infected patients and to establish hepatitis in chimeric mice. However, we rarely detected tetramer-positive CTLs in blood samples from chronically infected patients and were therefore unable to establish hepatitis using CD8-positive T cells. Consequently, a limitation of this study is that differential roles of NK cells and CTLs in massive liver cell death could not be examined.

Although it is not clear in this study how profoundly DC and NK cell activity plays a role in patients with FHB, our results suggest that the immune system can trigger severe hepatocyte

degeneration. The importance of the activation of NK cells by DCs was evident, because depletion of DCs almost completely abolished the massive hepatocyte degeneration in this model (Supporting Fig. 10; Table 1). The interaction between NK cells and DCs is not well characterized, although it has been established that antigen-presenting accessory cells provide both indirect (i.e., soluble) and direct (i.e., contact-dependent) signals to T cells. Experiments in which NK cells are separated from pathogens and antigen-presenting cells by semipermeable membranes are cultured with supernatants from pathogen-activated DCs or in which cytokines are neutralized with blocking antibodies. These reports indicate that both soluble and contact-dependent signals may contribute to the activation of NK cells.[23,25,26]

The importance of the Fas/FasL system in hepatocyte damage in acute and chronic HBV infection has been reported previously.[37,38] However, the extent to which this system plays a role in human hepatitis B, especially fulminant hepatitis, is unknown. As shown in this study (Fig. 5A), inhibition of the Fas/FasL system by anti-Fas antibody dramatically reduced the effect of human PBMC transplantation. This showed the possibility that the Fas/FasL system plays an important role in the degeneration of infected hepatocytes in FHB. Further studies should be conducted to evaluate what immunological responses play important roles in human hepatitis B.

The importance of NK-cell activity suggests that the suppression of DCs and NK-cell activity or the Fas/FasL system might have therapeutic implications for FHB.[11,35] If DCs and NK-cell activity or Fas/FasL activity could be controlled in the early stages of severe acute or fulminant hepatitis, we might be able to control hepatitis activity and prevent subsequent liver failure. Of course, it would be necessary to monitor the development of chronic hepatitis after such treatment because DCs and NK cells contribute to early host defenses and shape subsequent adaptive immune response through complex cross-talk regulating the early phase of the immune response.[19,24,39,40]

We analyzed liver damage using HBV genotype C–infected mice in this study. However, HBV genotype C is associated with more severe histological liver damage than genotype B,[41] and future studies should compare immunological differences between genotypes B and C.

In summary, we established an animal model of FHB using highly repopulated human hepatocyte chimeric mice and transplanted human PBMCs. Modifications of this model will facilitate further research into acute and CHB using human immune cells, including HBV-directed CTL clones, suppressor and regulatory T cells, as well as immunological experiments to study interactions between DCs and NK cells. Such models may be useful to develop and evaluate new therapeutic strategies against HBV infection.

Acknowledgment: The authors thank Rie Akiyama and Yoko Matsumoto for their expert technical assistance. This work was carried out at the Analysis Center of Life Science, Natural Science Center for Basic Research and Development, Hiroshima University.

References

1. Bernal W, Auzinger G, Dhawan A, Wendon J. Acute liver failure. Lancet 2010;376:190-201.
2. Leifeld L, Cheng S, Ramakers J, Dumoulin FL, Trautwein C, Sauerbruch T, Spengler U. Imbalanced intrahepatic expression of interleukin 12, interferon gamma, and interleukin 10 in fulminant hepatitis B. HEPATOLOGY 2002;36:1001-1008.
3. Ozasa A, Tanaka Y, Orito E, Sugiyama M, Kang JH, Hige S, et al. Influence of genotypes and precore mutations on fulminant or chronic outcome of acute hepatitis B virus infection. HEPATOLOGY 2006;44: 326-334.
4. Kawai T, Akira S. Toll-like receptor and RIG-I-like receptor signaling. Ann N Y Acad Sci 2008;1143:1-20.
5. Maini MK, Boni C, Lee CK, Larrubia JR, Reignat S, Ogg GS, et al. The role of virus-specific CD8(+) cells in liver damage and viral control during persistent hepatitis B virus infection. J Exp Med 2000;191: 1269-1280.
6. Guidotti LG, Ando K, Hobbs MV, Ishikawa T, Runkel L, Schreiber RD, Chisari FV. Cytotoxic T lymphocytes inhibit hepatitis B virus gene expression by a noncytolytic mechanism in transgenic mice. Proc Natl Acad Sci U S A 1994;91:3764-3768.
7. Ando K, Moriyama T, Guidotti LG, Wirth S, Schreiber RD, Schlicht HJ, et al. Mechanisms of class I restricted immunopathology. A transgenic mouse model of fulminant hepatitis. J Exp Med 1993;178: 1541-1554.
8. Cote PJ, Toshkov I, Bellezza C, Ascenzi M, Roneker C, Ann Graham L, et al. Temporal pathogenesis of experimental neonatal woodchuck hepatitis virus infection: increased initial viral load and decreased severity of acute hepatitis during the development of chronic viral infection. HEPATOLOGY 2000;32:807-817.
9. Chisari FV. Rous-Whipple Award Lecture. Viruses, immunity, and cancer: lessons from hepatitis B. Am J Pathol 2000;156:1117-1132.
10. Dunn C, Brunetto M, Reynolds G, Christophides T, Kennedy PT, Lampertico P, et al. Cytokines induced during chronic hepatitis B virus infection promote a pathway for NK cell-mediated liver damage. J Exp Med 2007;204:667-680.
11. Zhang Z, Zhang S, Zou Z, Shi J, Zhao J, Fan R, et al. Hypercytolytic activity of hepatic natural killer cells correlates with liver injury in chronic hepatitis B patients. HEPATOLOGY 2011;53:73-85.
12. Dandri M, Burda MR, Torok E, Pollok JM, Iwanska A, Sommer G, et al. Repopulation of mouse liver with human hepatocytes and *in vivo* infection with hepatitis B virus. HEPATOLOGY 2001;33:981-988.
13. Petersen J, Burda MR, Dandri M, Rogler CE. Transplantation of human hepatocytes in immunodeficient UPA mice: a model for the study of hepatitis B virus. Methods Mol Med 2004;96:253-260.
14. Ogata N, Miller RH, Ishak KG, Purcell RH. The complete nucleotide sequence of a pre-core mutant of hepatitis B virus implicated in fulminant hepatitis and its biological characterization in chimpanzees. Virology 1993;194:263-276.

15. Tateno C, Yoshizane Y, Saito N, Kataoka M, Utoh R, Yamasaki C, et al. Near completely humanized liver in mice shows human-type metabolic responses to drugs. Am J Pathol 2004;165:901-912.
16. Tsuge M, Hiraga N, Takaishi H, Noguchi C, Oga H, Imamura M, et al. Infection of human hepatocyte chimeric mouse with genetically engineered hepatitis B virus. HEPATOLOGY 2005;42:1046-1054.
17. Tsuge M, Hiraga N, Akiyama R, Tanaka S, Matsushita M, Mitsui F, et al. HBx protein is indispensable for development of viraemia in human hepatocyte chimeric mice. J Gen Virol 2010;91:1854-1864.
18. Kuhober A, Pudollek HP, Reifenberg K, Chisari FV, Schlicht HJ, Reimann J, Schirmbeck R. DNA immunization induces antibody and cytotoxic T cell responses to hepatitis B core antigen in H-2b mice. J Immunol 1996;156:3687-3695.
19. Banchereau J, Steinman RM. Dendritic cells and the control of immunity. Nature 1998;392:245-252.
20. Shortman K, Liu YJ. Mouse and human dendritic cell subtypes. Nat Rev Immunol 2002;2:151-161.
21. Sandhu J, Shpitz B, Gallinger S, Hozumi N. Human primary immune response in SCID mice engrafted with human peripheral blood lymphocytes. J Immunol 1994;152:3806-3813.
22. Gonzalez SF, Lukacs-Kornek V, Kuligowski MP, Pitcher LA, Degn SE, Kim YA, et al. Capture of influenza by medullary dendritic cells via SIGN-R1 is essential for humoral immunity in draining lymph nodes. Nat Immunol 2010;11:427-434.
23. Fernandez NC, Lozier A, Flament C, Ricciardi-Castagnoli P, Bellet D, Suter M, et al. Dendritic cells directly trigger NK cell functions: cross-talk relevant in innate anti-tumor immune responses *in vivo*. Nat Med 1999;5:405-411.
24. Ferlazzo G, Tsang ML, Moretta L, Melioli G, Steinman RM, Munz C. Human dendritic cells activate resting natural killer (NK) cells and are recognized via the NKp30 receptor by activated NK cells. J Exp Med 2002;195:343-351.
25. Andoniou CE, van Dommelen SL, Voigt V, Andrews DM, Brizard G, Asselin-Paturel C, et al. Interaction between conventional dendritic cells and natural killer cells is integral to the activation of effective antiviral immunity. Nat Immunol 2005;6:1011-1019.
26. Walzer T, Dalod M, Robbins SH, Zitvogel L, Vivier E. Natural-killer cells and dendritic cells: "l'union fait la force". Blood 2005;106:2252-2258.
27. Mosier DE, Gulizia RJ, Baird SM, Wilson DB, Spector DH, Spector SA. Human immunodeficiency virus infection of human-PBL-SCID mice. Science 1991;251:791-794.
28. Kawahara T, Douglas DN, Lewis J, Lund G, Addison W, Tyrrell DL, et al. Critical role of natural killer cells in the rejection of human hepatocytes after xenotransplantation into immunodeficient mice. Transpl Int 2010;23:934-943.
29. Morosan S, Hez-Deroubaix S, Lunel F, Renia L, Giannini C, Van Rooijen N, et al. Liver-stage development of *Plasmodium falciparum*, in a humanized mouse model. J Infect Dis 2006;193:996-1004.
30. Dorshkind K, Pollack SB, Bosma MJ, Phillips RA. Natural killer (NK) cells are present in mice with severe combined immunodeficiency (SCID). J Immunol 1985;134:3798-3801.
31. Ito M, Hiramatsu H, Kobayashi K, Suzue K, Kawahata M, Hioki K, et al. NOD/SCID/gamma(c)(null) mouse: an excellent recipient mouse model for engraftment of human cells. Blood 2002;100:3175-3182.
32. Thimme R, Wieland S, Steiger C, Ghrayeb J, Reimann KA, Purcell RH, Chisari FV. CD8(+) T cells mediate viral clearance and disease pathogenesis during acute hepatitis B virus infection. J Virol 2003;77:68-76.
33. Rehermann B, Fowler P, Sidney J, Person J, Redeker A, Brown M, et al. The cytotoxic T lymphocyte response to multiple hepatitis B virus polymerase epitopes during and after acute viral hepatitis. J Exp Med 1995;181:1047-1058.
34. Webster GJ, Reignat S, Maini MK, Whalley SA, Ogg GS, King A, et al. Incubation phase of acute hepatitis B in man: dynamic of cellular immune mechanisms. HEPATOLOGY 2000;32:1117-1124.
35. Zou Y, Chen T, Han M, Wang H, Yan W, Song G, et al. Increased killing of liver NK cells by Fas/Fas ligand and NKG2D/NKG2D ligand contributes to hepatocyte necrosis in virus-induced liver failure. J Immunol 2010;184:466-475.
36. Newman KC, Riley EM. Whatever turns you on: accessory-cell-dependent activation of NK cells by pathogens. Nat Rev Immunol 2007;7:279-291.
37. Galle PR, Hofmann WJ, Walczak H, Schaller H, Otto G, Stremmel W, et al. Involvement of the CD95 (APO-1/Fas) receptor and ligand in liver damage. J Exp Med 1995;182:1223-1230.
38. Rivero M, Crespo J, Fábrega E, Casafont F, Mayorga M, Gomez-Fleitas M, Pons-Romero F. Apoptosis mediated by the Fas system in the fulminant hepatitis by hepatitis B virus. J Viral Hepat 2002;9:107-113.
39. Moretta A. Natural killer cells and dendritic cells: rendezvous in abused tissues. Nat Rev Immunol 2002;2:957-964.
40. Asselin-Paturel C, Trinchieri G. Production of type I interferons: plasmacytoid dendritic cells and beyond. J Exp Med 2005;202:461-465.
41. Orito E, Ichida T, Sakugawa H, Sata M, Horiike N, Hino K, et al. Geographic distribution of hepatitis B virus (HBV) genotype in patients with chronic HBV infection in Japan. HEPATOLOGY 2001;34:590-594.

ORIGINAL ARTICLE

MicroRNA-221/222 upregulation indicates the activation of stellate cells and the progression of liver fibrosis

Tomohiro Ogawa,[1,2,3] Masaru Enomoto,[1] Hideki Fujii,[1] Yumiko Sekiya,[1,2] Katsutoshi Yoshizato,[2,4] Kazuo Ikeda,[5] Norifumi Kawada[1,2]

[1]Department of Hepatology, Graduate School of Medicine, Osaka City University, Osaka, Japan
[2]Liver Research Center, Graduate School of Medicine, Osaka City University, Osaka, Japan
[3]Center for the Advancement of Higher Education, Faculty of Engineering, Kinki University, Hiroshima, Japan
[4]PhoenixBio Co Ltd., Hiroshima, Japan
[5]Department of Anatomy and Cell Biology, Graduate School of Medicine, Nagoya City University, Aichi, Japan

Correspondence to
Professor Norifumi Kawada, Department of Hepatology, Graduate School of Medicine, Osaka City University, 1-4-3, Asahimachi, Abeno, Osaka 545-8585, Japan; kawadanori@med.osaka-cu.ac.jp

Revised 1 December 2011
Accepted 15 December 2011

Published Online First
20 January 2012

ABSTRACT

Background MicroRNAs (miRNAs) are important in hepatic pathophysiology and the development of liver cancer.

Objective To explore miRNAs that are regulated with the progression of liver fibrosis caused by chronic liver disease.

Design The regulated miRNAs in human livers infected with hepatitis C virus were identified by microarray analysis. Their expression in human livers with non-alcoholic steatohepatitis, mouse livers from two fibrosis models and cultured stellate cells was validated by real-time RT-PCR. The regulation of miR-222 expression in stellate cells by nuclear factor kappa B (NF-κB) was assayed. Finally, the effects of an miR-222 precursor or inhibitor on the expression of cyclin-dependent kinase inhibitor 1B (CDKN1B) and the growth of LX-2 cells were determined.

Results It was found that miR-199a-5p/199a-3p and miR-221/222 were upregulated in the human liver in a fibrosis progression–dependent manner. Among these miRNAs, miR-221/222 were upregulated in LX-2 cells and increased during the course of culture-dependent activation of mouse primary stellate cells, in a manner similar to the expression of α1(I) collagen and α-smooth muscle actin mRNAs. The expression of miR-221/222 increased in mouse models of liver fibrosis. In contrast, an NF-κB inhibitor significantly suppressed the miR-222 induction that was stimulated in culture by transforming growth factor α or tumour necrosis factor α. Although overexpression or downregulation of miR-222 failed to regulate the growth of LX-2 cells, miR-222 bound to the *CDKN1B* 3′UTR and regulated the expression of the corresponding protein.

Conclusion miR-221/222 may be new markers for stellate cell activation and liver fibrosis progression.

Significance of this study

What is already known about this subject?

- The abundance of miR-221/222 increases in human hepatocellular carcinoma (HCC).
- miR-221/222 elicit their oncogenic effects via the downregulation of tumour suppressors, such as p27, p57 and PTEN.
- The expression of miR-221/222 is induced by NF-κB activation in prostate carcinoma and glioblastoma cells.

What are the new findings?

- The expression of miR-221/222 increases with the progression of human liver fibrosis and is correlated with the expression levels of α1 (I) collagen and α-smooth muscle actin mRNAs.
- The expression of miR-221/222 is highly correlated with α1 (I) collagen mRNA expression in mouse stellate cells in culture.
- miR-222 expression is inhibited by an NF-κB inhibitor and upregulated by NF-κB activators, such as tumour necrosis factor α and transforming growth factor α.

How might they impact on clinical practice in the foreseeable future?

- miR-221/222 have the potential to be new markers for stellate cell activation and liver fibrosis progression in humans.
- The pattern of miR-221/222 expression can serve as a useful tool for understanding and investigating the mechanism of the progression of liver fibrosis.
- The miRNA profiling of human liver fibrosis contributes to the identification of predictors of disease prognosis and potential therapeutic targets.

INTRODUCTION

Hepatic fibrosis is a consequence of the accumulation of extracellular matrix (ECM) components in the liver. This process is caused by the persistent liver damage and wound healing reaction induced by chronic viral hepatitis, alcohol abuse, non-alcoholic steatohepatitis (NASH) and several other aetiologies and can progress to cirrhosis and hepatocellular carcinoma (HCC).[1] Hepatitis C virus (HCV) infection is one of the leading causes of end-stage liver diseases worldwide and the most common indication for liver transplantation in the USA and Europe. In addition, non-alcoholic fatty liver disease and its progressive form, NASH, have become urgent clinical problems owing to the increasing prevalence of metabolic syndrome.[2–4] Because fibrotic liver disease has thus become a global health problem, it is important to understand the molecular mechanisms of hepatic fibrosis, irrespective of the cause, to establish proper therapeutic strategies and to identify diagnostic markers of this disease.

It is generally accepted that excessive production of ECM components by activated hepatic stellate cells and myofibroblasts is responsible for hepatic fibrosis.[5 6] Hepatic stellate cells exist in Disse's space and store vitamin A under physiological conditions.[7] When liver injury occurs, these cells become activated in response to oxidative stress, growth factors and inflammatory stimuli that are produced by damaged hepatocytes, resident macrophages (Kupffer cells), infiltrating inflammatory cells and aggregated platelets. The hepatic stellate cells then undergo transformation into myofibroblast-like cells that express α-smooth muscle actin (αSMA).[5] Activated stellate cells deposit ECM components, including types I and III collagen, fibronectin and laminin, at the site of local tissue damage and secrete profibrogenic mediators, such as transforming growth factor β (TGFβ), connective tissue growth factor and platelet-derived growth factor, thereby playing a pivotal role in liver fibrogenesis.[6]

MicroRNAs (miRNAs) are small, endogenous, non-coding RNAs that interact with the 3′ untranslated region (UTR) of target mRNAs, resulting in the inhibition of translation or the promotion of mRNA degradation.[8 9] miRNAs are important in proliferation,[10] development[11] and differentiation[12] in many cell types and are involved in the development of many diseases, including cancer.[13–15] miR-122 has been the best studied miRNA with regard to liver pathophysiology. For example, miR-122 is highly abundant in the human liver and is essential for HCV replication.[16–19] Interferon β rapidly modulates the expression of miR-122, which has sequence-predicted targets within the HCV RNA.[20] In chronic hepatitis C, decreased miR-122 has been associated with an absence of virological response to interferon and ribavirin treatment.[21] miR-21, -34a, -93, -96, -221/222 and -519a increase and, in contrast, let-7c decreases in human HCC.[22] The expression levels of miR-21 and miR-122 correlate with the histological evaluation of HCV-induced liver disease.[23]

Here, we show that the expression of miR-221/222 increased with the progression of liver fibrosis and significantly correlated with the expression of α1 (I) collagen (Col1A1) and αSMA mRNAs in human fibrotic livers. The expression of miR-221/222 in human fibrotic livers was also reproduced in mouse models of hepatic fibrosis. Interestingly, miR-221/222 were more highly expressed in a human stellate cell line, LX-2, than in HCC cell lines and their expression was induced with the activation of mouse stellate cells. Finally, we show that the expression of miR-222 in stellate cells may be regulated by the activation of nuclear factor kappa B (NF-κB). Taken together, our findings indicate that miR-221/222 upregulation is a new marker for stellate cell activation and liver fibrosis progression that could be used for the clinical diagnosis of liver fibrosis.

MATERIALS AND METHODS

Materials

Precursors and inhibitors of miR-222 and the negative control miRNA were purchased from Ambion (Austin, Texas, USA). Dulbecco's modified Eagle's medium (DMEM) and fetal bovine serum (FBS) were purchased from Sigma Chemical Co (St Louis, Missouri, USA). The mouse monoclonal antibody against cyclin-dependent kinase inhibitor 1B (CDKN1B (p27, Kip1)) was from Cell Signaling Technology Inc (Beverly, Massachusetts, USA) and that against glyceraldehyde 3-phosphate dehydrogenase (GAPDH) was from Chemicon International Inc (Temecula, California, USA). Enhanced Chemiluminescence Plus detection reagent was from GE Healthcare (Buckinghamshire, UK). Immobilon P membranes were from Millipore Corp. (Bedford, Massachusetts, USA). Recombinant human TGFα and mouse tumour necrosis factor (TNF)α were from R&D Systems, Inc (Minneapolis, Minnesota, USA). 6-Amino-4-(4-phenoxyphenylethylamono)quinazoline (QNZ) was from EMD Chemicals, Inc (Gibbstown, New Jersey, USA). All other reagents were purchased from Sigma Chemical Co or Wako Pure Chemical Co (Osaka, Japan).

Liver biopsy specimens

Liver biopsy specimens were obtained from 35 patients with chronic hepatitis C genotype 1 infection and 26 patients with NASH using a 15-gauge Tru-Cut biopsy needle (Hakko Inc., Tokyo, Japan) under ultrasound guidance (table 1). Of the 26 patients with NASH, oral hypoglycaemic agents were given to four patients (sulphonylureas to three and metformin to one), antihypertensive agents to eight (angiotensin receptor blockers to five and calcium channel blockers to three) and antihyperlipidaemic agents to eight (statins to five and fibrates to three) at the time of liver biopsy. Informed consent was obtained from all patients before biopsy. All procedures were in accordance with the Helsinki Declaration of 1975 (2008 revision). Biopsied liver tissues were fixed in 10% formalin solution and then embedded in paraffin. The stage of liver fibrosis was evaluated according to the METAVIR scoring system in patients with chronic hepatitis C[24] and the Brunt classification in patients with NASH.[4] A portion of each biopsy sample was immediately placed in RNAlater (Qiagen, Valencia, California, USA), temporarily stored at −20°C and then used to extract total RNAs using the mirVana miRNA Isolation Kit (Applied

Table 1 Baseline characteristics of patients

Characteristics	All patients with CHC (n=35)	Patients with CHC undergoing microarray analysis (n=22)	Patients with NASH (n=26)
Age (years)*	59±9	58±6	58±12
Female sex (%)†	20 (57)	11 (50)	14 (54)
Interferon-naïve (%)†	24 (69)	15 (68)	
ALT (IU/l)‡	57 (34–99)	88 (51–171)	69 (28–226)
Albumin (g/dl)*	4.0±0.3	4.0±0.3	4.0±0.5
Platelet count ($\times 10^9$/l)*	179±53	169±46	184±54
HCV RNA ($\log_{10}$ copies/ml)*	6.1±1.0	6.0±1.2	
Grade of necroinflammation† (A0/A1/A2/A3)	3/23/8/1	2/13/6/1	0/10/10/6
Stage of fibrosis† (F1/F2/F3/F4)	19/7/7/2	11/4/5/2	7/8/8/3

*Mean±SD.
†Numbers of patients.
‡Median (IQR).
ALT, alanine aminotransferase; CHC, chronic hepatitis C; HCV, hepatitis C virus; NASH, non-alcoholic steatohepatitis.

Biosystems, Foster City, California, USA). As controls, normal liver tissues were taken from four patients who underwent resection for metastatic liver tumours.

Microarray analysis

In 22 of the 35 patients with chronic hepatitis C and in four controls, microarray analysis was performed using 10 μg total RNA with the 3D-Gene Human miRNA Oligo chip v10.1 (Toray, Tokyo, Japan), as described in detail elsewhere.[25]

Mouse model of liver fibrosis

Male C57BL/6 mice, 7–10 weeks old, were purchased from Japan SLC, Inc (Shizuoka, Japan). All animals received humane care. The experimental protocol was approved by the Committee of Laboratory Animals according to institutional guidelines. Mice (n=5) were injected intraperitoneally with 200 μg/g body weight of thioacetamide (TAA, Sigma) diluted in saline three times a week for 4 or 8 weeks.[26] Control mice (n=5) were injected with saline. As another liver fibrosis model, mice were given either a methionine- and choline-deficient diet (MCDD, n=7) or methionine-choline control diet (MCCD, n=7) for 5 or 15 weeks, as previously described.[27] In addition, a similar model was generated in rats by giving them MCCD for 10 weeks, MCDD for 10 weeks, or MCDD for 8 weeks followed by MCCD for the last 2 weeks (recovery group).[27] The ingredients for these diets were purchased from MP Biomedicals (Solon, Ohio, USA).

Cells

Primary stellate cells were isolated from male C57BL/6 mice by the pronase-collagenase digestion method[28] and were cultured in DMEM supplemented with 10% FBS. Hepatocytes were isolated by collagenase digestion. One day after culturing, the cells were treated with TGFα (1–10 ng/ml), TNFα (0.1–1 ng/ml), or QNZ (10–100 nmol/l) for 24 or 72 h. LX-2 (donated by Dr Scott Friedman[29]), NIH3T3 and Huh7 cells were maintained on plastic culture plates in DMEM supplemented with 10% FBS. HepG2 cells (JCRB1054), obtained from the Health Science Research Resources Bank (Osaka, Japan), were maintained on plastic culture plates in Minimum Essential Medium (Invitrogen, Carlsbad, California, USA) supplemented with 10% FBS, 1 mM sodium pyruvate (Invitrogen) and 1% non-essential amino acids (Invitrogen).

Quantitative real-time PCR

Total RNA was extracted from cells and liver tissues using the miRNeasy Mini Kit (Qiagen). cDNAs were synthesised using 0.5 μg of total RNA, a ReverTra Ace qPCR RT Kit (Toyobo, Osaka, Japan) and oligo(dT)$_{12-18}$ primers, according to the manufacturer's instructions. Gene expression was measured by real-time PCR using the cDNAs, THUNDERBIRD SYBR qPCR Mix Reagents (Toyobo) and gene-specific oligonucleotide primers (listed in table 2) with an ABI Prism 7500 Real-Time PCR System (Applied Biosystems). The GAPDH level was used to normalise the relative abundance of mRNAs. To detect miRNA expression, the RT reaction was performed using the TaqMan MicroRNA Assay (Applied Biosystems). Primers for PCR reactions in the miRNA assays were obtained from Applied Biosystems.

Immunoblotting

Proteins (20 μg) were subjected to sodium dodecyl sulphate–polyacrylamide gel electrophoresis and then transferred onto Immobilon P membranes. After blocking, the membranes were treated with primary antibodies followed by peroxidase-conjugated secondary antibodies. Immunoreactive bands were visualised by the enhanced chemiluminescence system using the Fujifilm Image Reader LAS-3000 (Fuji Medical Systems, Stamford, Connecticut, USA).

Table 2 List of primer sequences

Gene		Sequence (5′-3′)	Accession No
Human	Forward	CCCGGGTTTCAGAGACAACTTC	NM_000088
Col1A1	Reverse	TCCACATGCTTTATTCCAGCAATC	
Human	Forward	GACAATGGCTCTGGGCTCTGTAA	NM_001613
αSMA	Reverse	CTGTGCTTCGTCACCCACGTA	
Human	Forward	AGCTTGCCCGAGTTCTACTACAG	NM_004064
CDKN1B	Reverse	ACCAAATGCGTGTCCTCAGAGT	
Human	Forward	CTCTACTGGCGAAACCTGTATCC	NM_000089
Col1A2	Reverse	TCTCCTAGCCAGACGTGTTTCTT	
Human	Forward	CTGGCCACAACTGCCAAATG	NM_001145938
MMP1	Reverse	CTGTCCCTGAACAGCCCAGTACTTA	
Human	Forward	TGACATCAAGGGCATTCAGGAG	NM_001127891
MMP2	Reverse	TCTGAGCGATGCCATCAAATACA	
Human	Forward	TCGAACTTTGACAGCGACAAGAA	NM_004994
MMP9	Reverse	TCAGTGAAGCGGTACATAGGGTACA	
Human	Forward	GGATACTTCCACAGGTCCCACAA	NM_003254
TIMP1	Reverse	CTGCAGGTAGTGATGTGCAAGAGTC	
Human	Forward	GGAGCACTGTGTTTATGCTGGAA	NM_003255
TIMP2	Reverse	GACCGAGCGATTGCTCAAGA	
Human	Forward	AGCGACTCGCCAGAGTGGTTA	NM_000660
TGFβ1	Reverse	GCAGTGTGTTATCCCTGCTGTCA	
Human	Forward	GCACCGTCAAGGCTGAGAAC	NM_002046
GAPDH	Reverse	TGGTGAAGACGCCAGTGGA	
Mouse	Forward	CCTGGCAAAGACGGACTCAAC	NM_007742
Col1A1	Reverse	GCTGAAGTCATAACCGCCACTG	
Mouse	Forward	TCCCTGGAGAAGAGCTACGAACT	NM_007392
αSMA	Reverse	AAGCGTTCGTTTCCAATGGT	
Mouse	Forward	TGCACCACCAACTGCTTAG	NM_008084
GAPDH	Reverse	GGATGCAGGGATGATGTTC	

Col1A1, α1 (I) collagen; GAPDH, glyceraldehyde 3-phosphate dehydrogenase; MMP, matrix metalloproteinase; αSMA, α-smooth muscle actin; TIMP, tissue inhibitor of matrix metalloproteinase.

Transient transfection with miRNA precursors and inhibitors

Precursors or inhibitors of miR-222 and the negative control miRNA were transfected into human and mouse stellate cells using Lipofectamine RNAiMAX Transfection Reagent (Invitrogen) at a final concentration of 50 nmol/l, as previously described.[30 31] After 6 h, the culture medium was changed. Then, after 24 h, the cells were collected for total RNA and protein extraction.

Luciferase reporter assay

The interaction of the *CDKN1B* 3′UTR with miR-222 was assayed basically according to a previously described method.[30 31] The *CDKN1B* 3′UTR was obtained by PCR using human stellate cell cDNA as a template and the primer set forward 5′-TTCTCGAGGTTCTTGTCTTGATGTGTCACC-3′, reverse 5′-TTTCTAGAGAGAGCAGAGGCCTGAGAAG-3′. The Dual-Glo Luciferase Assay System (Promega, Madison, Wisconsin, USA) was used to analyse luciferase expression, according to the manufacturer's protocol.

Cell proliferation assay

LX-2 cells were plated at a density of 3×10^3 cells/well in 96-well plates for 24 h and were then transfected with the miR-222 precursor or inhibitor as described above. After 24 h, the medium was changed and culturing was continued for an additional

1–3 days before measuring cell proliferation by the WST-1 assay.[31]

Statistical analysis

Data, presented as box plots, are the median, IQR, minimum and maximum. The Mann–Whitney U test was used to analyse the distribution of continuous variables. The Jonckheere–Terpstra test for ordered alternatives was used to identify trends among classes. Correlation coefficients between parameters were evaluated by Spearman rank correlations. A two-tailed p value <0.05 was considered significant.

RESULTS

Patient characteristics

Table 1 shows the baseline characteristics of the patients infected with HCV and those with NASH who were included in this study. There were no significant differences in clinical, biochemical, haematological, virological, or histological characteristics between the 22 patients with HCV who were analysed by microarray and the 13 patients with HCV who were not.

miRNA expression profile in patients with HCV

We comprehensively compared miRNA expression profiles between cases of mild liver fibrosis (F1/F2) and advanced liver fibrosis (F3/F4) among the 22 patients with HCV using microarray analysis. As shown in the heat map in figure 1, 18 miRNAs were significantly upregulated (fold change, 1.21 to 2.59), whereas six miRNAs were significantly downregulated (fold change, −1.69 to −1.20) in livers with advanced fibrosis. Among the 18 overexpressed miRNAs, p values of <0.01 were found for miR-222 (fold change, 1.80), miR-214 (fold change, 1.84), miR-199a-3p (miR-199b-3p) (fold change, 1.90) and miR-199a-5p (fold change, 2.00). Among the six downregulated miRNAs, miR-422a (fold change, −1.69) showed a p value <0.01. Among them, the abundance of miR-199a-5p and miR-199a-3p has previously been reported to be increased in fibrotic liver disease.[32]

Next, we quantitatively confirmed our miRNA expression results in 35 patients with HCV (table 1) using real-time PCR. miR-199a-5p, miR-199a-3p and miR-222 were significantly upregulated in a stepwise manner according to the progression of liver fibrosis (figure 2A). miR-222 forms a cluster with miR-221 in the human and mouse genomes. In fact, miR-221 expression was significantly upregulated in patients with HCV with severe fibrosis (figure 2A). Col1A1 mRNA expression also significantly increased with increasing progression of liver fibrosis (figure 2B) and was significantly correlated with the expression of miR-222 ($r=0.843$, $p<0.001$) (figure 2C). Additionally, αSMA mRNA expression tended to increase according to the progression of fibrosis (figure 2B) and was significantly correlated with the expression of miR-222 ($r=0.701$, $p<0.001$) (figure 2C).

MicroRNA-221/222 expression in patients with NASH

We also validated miR-221 and miR-222 expression in 26 patients with biopsy-proven NASH (F1, seven; F2, eight; F3, eight; F4, three) by real-time PCR. The expression of these miRNAs was significantly upregulated in a manner dependent on the progression of liver fibrosis (figure 3A). Col1A1 mRNA expression was also significantly upregulated (figure 3B) and correlated with the expression of miR-222 ($r=0.626$, $p<0.001$) (figure 3C). In contrast, the expression level of αSMA mRNA tended towards a correlation with that of miR-222, but this result was not significant ($r=0.375$, $p=0.059$) (figure 3B,C). These results indicate the close correlation between miR-222 and Col1A1 mRNA expression in human liver fibrosis caused by NASH.

Expression of miR-221/222 in rodent models of liver fibrosis

Next, we studied miR-221 and miR-222 expression in mouse models of liver fibrosis. First, liver fibrosis was induced in mice by injecting TAA for 8 weeks. As shown in figure 4A, haematoxylin and eosin staining and Sirius red staining confirmed the occurrence of liver fibrosis, in particular around the central vein

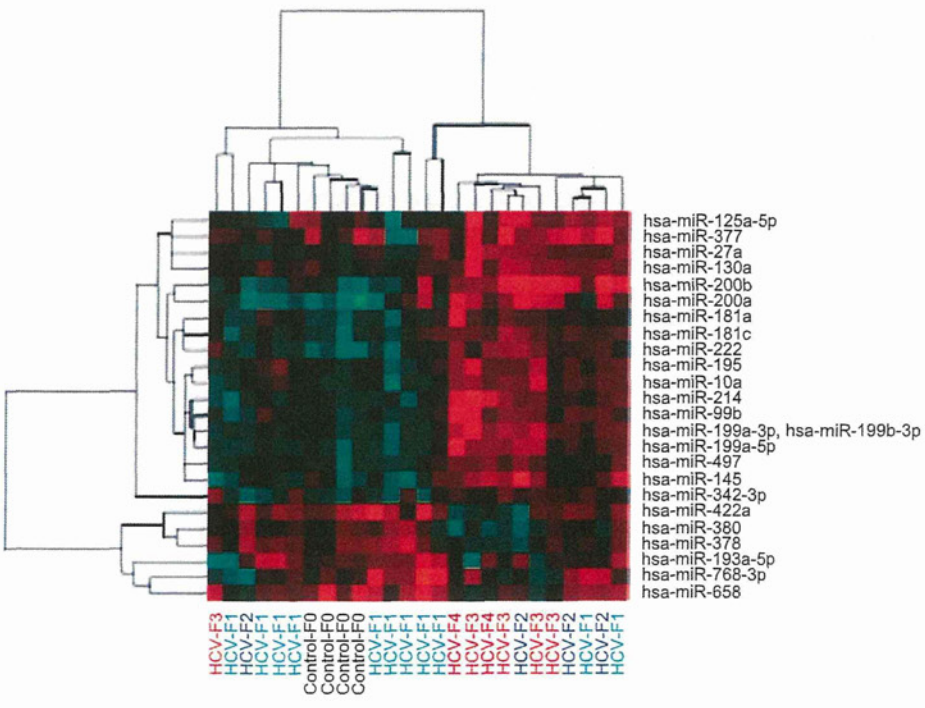

Figure 1 Heat map of microRNA (miRNA) expression in human liver tissue. Shown is the clustering of patients (n=22) with chronic hepatitis C by comprehensive analysis of intrahepatic miRNA expression according to the degree of hepatic fibrosis in biopsy specimens. Green and red denote downregulated and upregulated genes, respectively. F, fibrosis stage; HCV, hepatitis C virus.

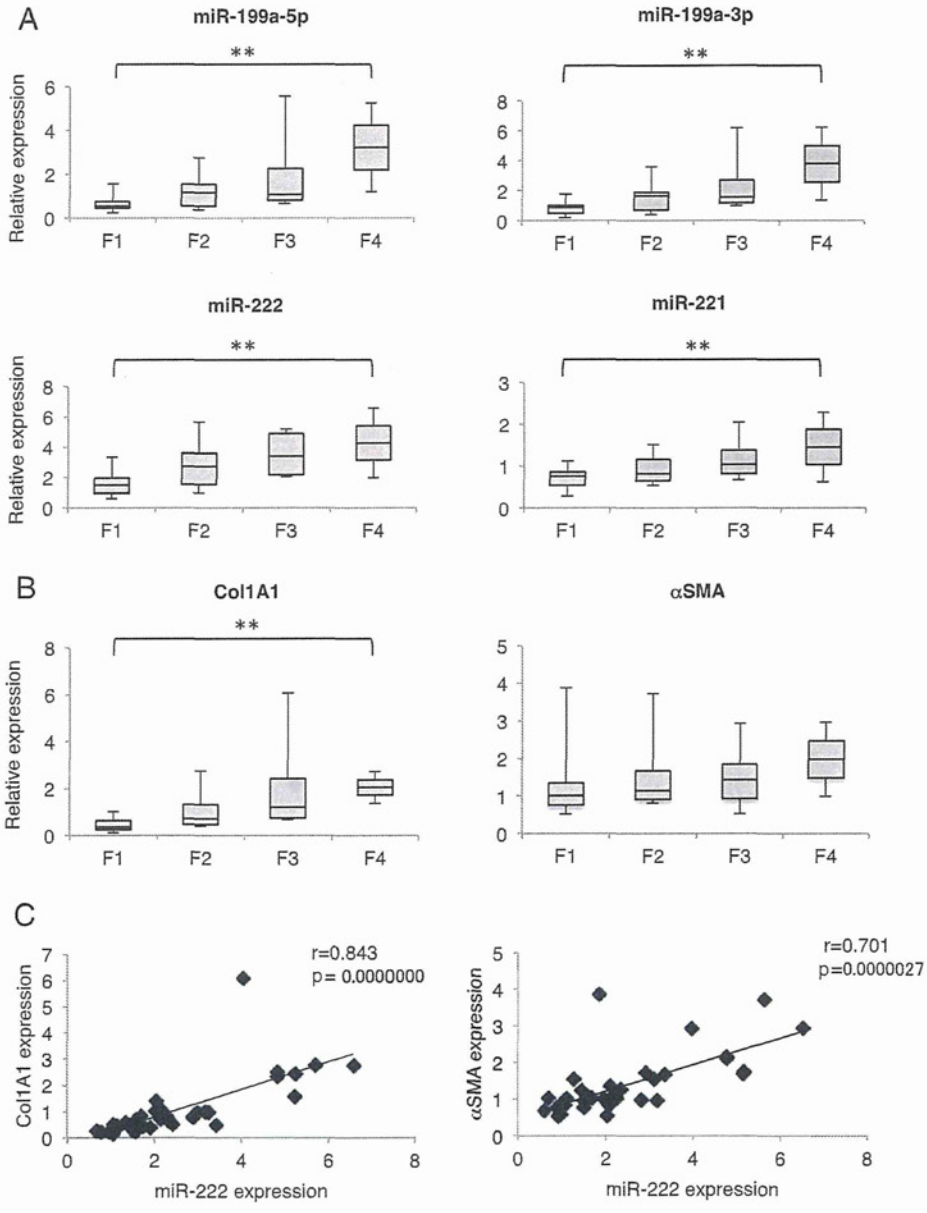

Figure 2 MicroRNA (miRNA) levels and their correlations with Col1A1 and α-smooth muscle actin (αSMA) mRNA expression in patients with chronic hepatitis C. (A) Expression of miR-199a-5p, miR-199a-3p, miR-222 and miR-221 in 35 patients with hepatitis C virus (HCV) with fibrosis. The expression levels are indicated relative to F1. The Jonckheere–Terpstra test for ordered alternatives was used to identify trends among classes. **p<0.01. (B) Expression of Col1A1 and αSMA mRNAs in 35 patients with HCV with fibrosis. The expression levels are indicated relative to F1. Glyceraldehyde 3-phosphate dehydrogenase was used as an internal control. The Jonckheere–Terpstra test for ordered alternatives was used to identify trends among classes. **p<0.01. (C) Correlation between miR-222 expression and Col1A1 or αSMA mRNA expression. Correlation coefficients between parameters were evaluated by Spearman rank correlations.

area. These mouse livers exhibited significant upregulation of the expression of Col1A1 (3.1-fold, p<0.05) and αSMA (1.9-fold, p<0.05) mRNAs compared with the control livers at 8 weeks (figure 4B). The expression of miR-221 and miR-222 increased by 1.8-fold (p=0.06) and 1.4-fold (p<0.01), respectively, at 8 weeks after TAA injection (figure 4C). The increased expression of miR-222 was accompanied by increased Col1A1 (p<0.05) and αSMA mRNA expression (p<0.01) (data not shown). Another liver fibrosis model was produced in mice by feeding them an MCDD. miR-221 and miR-222 increased by 2.4-fold (p<0.01) and 2.6-fold (p<0.01), respectively, in livers of mice fed MCDD for 15 weeks compared with those fed MCCD for 15 weeks (figure 4D). These results confirm that the increased expression of miR-221/222 in fibrotic livers is reproduced in mouse models. In addition, miR-221 and miR-222 expression increased in rats administered MCDD for 10 weeks, but returned to the level of the controls after 2 weeks on MCCD in the recovery group (figure 4E). These data clearly indicate the correlation between the increase in miR-221/222 and liver fibrosis.

Expression of miR-222 in hepatic stellate cells

According to the data obtained from human and rodent fibrotic livers, we assumed that stellate cells may contribute to the increases of miR-222 and its homologue miR-221. As expected, the expression of both miR-221 and miR-222 increased during the activation process of mouse stellate cells in primary culture (6.1- and 26.8-fold increases in miR-221 and 4.1- and 13.9-fold increases in miR-222 at day 4 and day 7 compared with day 1, respectively), in a manner similar to the mRNA expression of Col1A1 and αSMA (38.3- and 61.3-fold increases in Col1A1 mRNA and 6.1- and 6.9-fold increases in αSMA at day 4 and day 7 compared with day 1, respectively) (figure 5A,B). Isolated mouse hepatocytes expressed both miRNAs in smaller amounts than with the activated stellate cells (figure 5A). In addition, both miR-221 and miR-222 expression were significantly higher in LX-2 than in HepG2 cells (9.5- and 6.0-fold, respectively), Huh7 cells (9.2- and 4.4-fold, respectively) and NIH3T3 cells (1.1- and 3.2-fold, respectively) (figure 5C), confirming the relative specificity of the miRNA expression in activated stellate cells.

Gut 2012;**61**:1600–1609. doi:10.1136/gutjnl-2011-300717

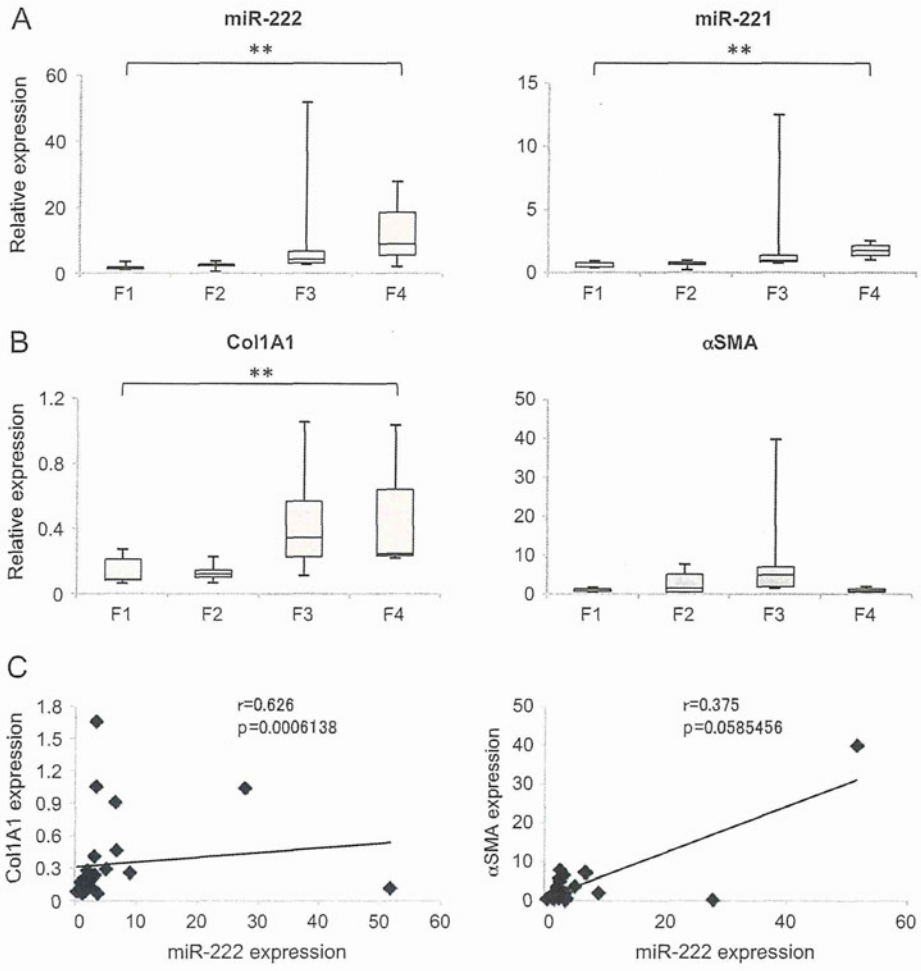

Figure 3 Levels of microRNA (miRNA)-221/222 and their correlation with Col1A1 and α-smooth muscle actin (αSMA) mRNA levels in patients with non-alcoholic steatohepatitis (NASH). (A) Expression of miR-221/222 in 26 patients with NASH. The expression levels are indicated relative to F1. The Jonckheere–Terpstra test for ordered alternatives was used to identify trends among classes. **p<0.01. (B) Expression of Col1A1 and αSMA mRNAs in 26 patients with NASH. The expression levels are indicated relative to F1. Glyceraldehyde 3-phosphate dehydrogenase was used as an internal control. The Jonckheere–Terpstra test for ordered alternatives was used to identify trends among classes. **p<0.01. (C) Correlation between miR-222 expression and Col1A1 or αSMA mRNA expression. Correlation coefficients between parameters were evaluated by Spearman rank correlations.

miR-222 transcription is regulated by NF-κB; the genomic region upstream of human miR-222 has multiple NF-κB binding elements.[33] NF-κB regulates Col1A1 gene expression and stellate cell activation.[34–36] Thus, we studied whether NF-κB stimulators, such as TGFα and TNFα, induce miR-222 expression and, in contrast, whether an NF-κB inhibitor (QNZ) inhibits its expression. As shown in figure 5D, stimulation of stellate cells with TGFα (1 or 10 ng/ml) or TNFα (0.1 or 1 ng/ml) for 24 h from day 1 to day 2 upregulated miR-222 expression, while QNZ (10 or 100 nmol/l) significantly reduced it. Stimulation of stellate cells with TGFα (1 ng/ml) or TNFα (0.1 ng/ml) for 72 h from day 1 to day 4 upregulated miR-222 expression by 1.9-fold (p<0.01) or 1.3-fold (p<0.05), respectively, compared with the untreated control (figure 5E) and miR-222 upregulation was inhibited to 18% or 26% of the untreated control level, respectively, by QNZ (figure 5E). These results indicate that miR-222 expression in stellate cells is regulated by NF-κB activation. QNZ (10 nmol/l) inhibited the activation-associated morphological transition of mouse hepatic stellate cells (figure 5F). This condition attenuated the expression of Col1A1 mRNA to 21% (p<0.01) and αSMA mRNA to 63% (p<0.01) of the untreated control levels (figure 5G).

Interaction of miR-222 with the *CDKN1B* 3′UTR in human stellate cells

miR-221 controls CDKN1B and CDKN1C expression in HCC cell lines.[37] The prediction of miRNA target regions by TargetScan (http://www.targetscan.org/) indicated that the *CDKN1B* 3′UTR has two target regions for miR-221/222 (figure 6A). Here, we investigated the presence of a direct interaction between miR-222 and CDKN1B mRNA in LX-2 cells by the firefly luciferase reporter assay and found that the miR-222 precursors inhibited luciferase activity derived from vectors carrying the *CDKN1B* 3′UTR (figure 6B). These observations indicate that the *CDKN1B* 3′UTR could be targeted by miR-222 in LX-2 cells.

Next, we transfected miR-222 precursors and miR-222 inhibitors into LX-2 cells. The transient transfection of miR-222 precursors significantly inhibited CDKN1B mRNA and protein expression compared with their expression in cells transfected with the negative control miRNA (figure 6C). Additionally, the transfection of miR-222 inhibitors significantly upregulated CDKN1B mRNA and protein expression in comparison with cells transfected with the negative control miRNA (figure 6D). Even though the transfection of miR-222 precursors or inhibitors into LX-2 cells showed negligible effects on cell growth (figure 6E,F), these results indicate that miR-222 targets *CDKN1B* in LX-2 cells.

Additional analyses indicated that transient transfection with miR-222 precursors significantly upregulated Col1A1 and matrix metalloproteinase 2 (MMP-2) mRNA expression and downregulated MMP-1, MMP-9 and TGFβ1 mRNA expression via unknown mechanisms (figure 6G).

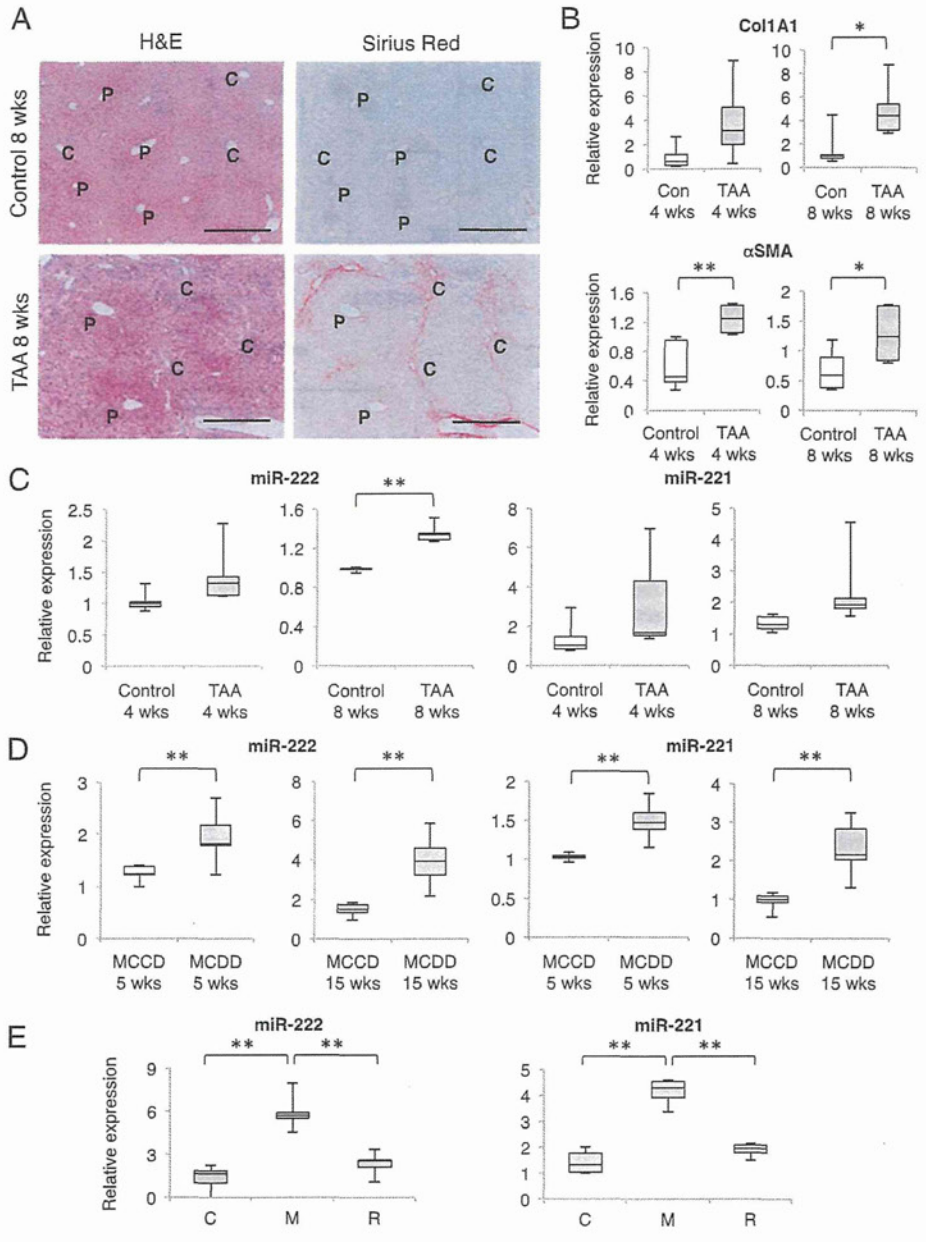

Figure 4 Expression of miR-221/222 in mouse models of liver fibrosis. (A) Liver fibrosis was induced in mice by injecting 200 μg/g body weight of thioacetamide (TAA) for 8 weeks. Haematoxylin and eosin staining (H&E; left). Sirius red staining (right). Scale bars, 200 μm. C, central vein area; P, portal vein area. (B) mRNA expression of Col1A1 and α-smooth muscle actin (αSMA) in TAA-induced liver fibrosis. The expression levels are indicated relative to control livers. Glyceraldehyde 3-phosphate dehydrogenase was used as an internal control. *p<0.05, **p<0.01 compared with control. (C) Expression of miR-221 and miR-222 in TAA-induced liver fibrosis. The expression levels are indicated relative to control livers. **p<0.01 compared with control. In B and C, open columns indicate data from controls and closed columns from TAA. (D) Expression of miR-221 and miR-222 in a methionine- and choline-deficient diet (MCDD)-induced liver fibrosis. The expression levels are indicated relative to methionine-choline control diet (MCCD) mouse livers. **p<0.01 compared with MCCD. Open columns indicate data from MCCD and closed columns from MCDD. (E) Expression of miR-221 and miR-222 in MCDD-induced liver fibrosis in rats.[27] The expression levels are indicated relative to rats fed MCCD for 10 weeks (C). Liver miR-221 and miR-222 levels significantly decreased in the recovery phase (R, MCDD for 8 weeks followed by MCCD for 2 weeks) compared with those fed MCDD for 10 weeks (M). **p<0.01.

DISCUSSION

Our study explored miRNA expression profiles during the progression of liver fibrosis in patients infected with HCV using microarray analysis. The expression of miR-222 was significantly correlated with that of Col1A1 and αSMA mRNAs in patients with HCV and with the expression of miR-221. To our knowledge, this is the first report to identify miR-221 and miR-221 as fibrosis-related molecules and to report miR-221/222 expression in a liver pathology other than carcinogenesis. Our results additionally indicate the close correlation between miR-221/222 and Col1A1 mRNA expression in the livers of people with NASH.

Recently, Roderburg *et al* reported the upregulation of miR-125-5p, miR-199b-3p, miR-221 and miR-302 and the downregulation of miR-29 family members in CCl_4-treated mouse livers, as observed using microarray analysis and quantitative RT-PCR.[38] Murakami *et al* reported that increased miR-199a-5p, miR-199a-3p, miR-200a and miR-200b levels are significantly associated with the progression of liver fibrosis in both humans and mice and that the overexpression of miR-199a-3p in human stellate cells results in the significant induction of tissue inhibitor of MMP-1, Col1A1 and MMP-13.[32] Furthermore, the expression levels of miR-21 and miR-122 have been correlated with the histological findings of HCV-induced liver disease.[23] However, in our analyses, although the expression of miR-199a-5p, miR-199a-3p and miR-21 tended to increase in activated mouse stellate cells during culture (0.8- and 2.1-fold for miR-199a-5p, 0.7- and 1.5-fold for miR-199a-3p and 1.9- and 3.8-fold for miR-21 at day 4 and day 7, respectively, compared with day 1), they failed to increase more than 10-fold, as miR-221 and miR-222 did (data not shown). Thus, miR-222 and miR-221 are more likely to reflect the activation of stellate cells than miR-199a-5p, miR-199a-3p and miR-21, similarly to the expression of Col1A1 mRNA.

It is generally accepted that liver fibrosis is a major risk factor for the development of HCC. A national surveillance